Inorg. Chem. **2004**, *43*, 2654–2671

Electronic Structure and Spectra of Linkage Isomers of Bis(bipyridine)(1,2-dihydroxy-9,10-anthraquinonato)ruthenium(II) and Their Redox Series

Antonietta DelMedico,[†] Elaine S. Dodsworth,* A. B. P. Lever,* and William J. Pietro

Department of Chemistry, York University, Toronto, Ontario, Canada M3J 1P3

Received November 26, 2003

Linkage isomers of bis(bipyridine)(1,2-dihydroxy-9,10-anthraquinonato)ruthenium(II), 1,2- and 1,9-coordinated complexes, and several of their oxidation products have been prepared chemically and/or electrochemically. For the 1,2-coordinated complex, the one- and two-electron oxidized species have been characterized, and for the 1,9-coordinated complex, the one-electron oxidized species has been characterized. The rich redox activity of these complexes leads to ambiguity in assessing the electronic structure. This paper reports EPR spectra of odd-electron species and detailed analyses of electronic spectra and structure of the complexes, based on INDO molecular orbital calculations. Results of calculations on the related 1-hydroxyanthraquinone complex and the free ligands,1,2-dihydroxy-9,10-anthraquinone (alizarin) and 1-hydroxyanthraquinone, are also briefly discussed.

Introduction

The bonding of ruthenium complexes containing redox-active dioxolene[1] and related ligands[2,3] has been an area of interest to our group for several years. Ruthenium complexes of dioxolenes have also been reported by others,[4] and there are several reviews covering complexes of other metals.[5] The term dioxolene is used to denote any member of the redox-related series catechol, semiquinone, quinone. These ligands are noninnocent[6] and thus can formally coordinate in any of their three oxidation states, and due to their valence orbitals lying close in energy to those of a number of the transition metals, they can form highly covalent complexes. This seems to be particularly true for complexes of ruthenium.[4,6] The 1,2-dihydroxy-9,10-anthraquinone (alizarin, $QcatH_2$) ligand which is discussed here is especially interesting because it combines both a *p*-quinone unit and an *o*-catechol.[2] Ruthenium complexes of some related hydroxyanthraquinones have also been reported.[7]

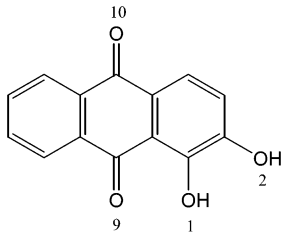

When alizarin is deprotonated and combined with the bis-(2,2′-bipyridine)ruthenium(II) fragment, complexes are obtained which have broad redox activity; both the alizarin and bipyridine (bpy) ligands are redox-active, as is the metal. Alizarin can be reduced stepwise by two electrons, formally at the 9,10-dioxo (*p*-quinone) unit, or it can be oxidized by two electrons at the 1,2-catechol-like (Cat) fragment to give *o*-semiquinone (*o*-Sq) and *o*-quinone (*o*-Q).[5,6,8] Under normal conditions the ruthenium(II) may be oxidized by one electron and each bipyridine may be reduced in two successive one-electron reduction processes.[9] The rich redox activity of these complexes leads to ambiguity in assessing their electronic

* To whom correspondence should be addressed. E-mail: dod@yorku.ca (E.S.D.); blever@yorku.ca (A.B.P.L.).

† Current address: Compliance Associates, 8000 Jane Street, Suite 103, Building B, Concord, Ontario, Canada L4K 5B8.

(1) (a) Haga, M.; Dodsworth, E. S.; Lever, A. B. P. *Inorg. Chem.* **1986**, *25*, 447. (b) Haga, M.; Dodsworth, E. S.; Lever, A. B. P.; Boone, S. R.; Pierpont, C. G. *J. Am. Chem. Soc.* **1986**, *108*, 7413. (c) Stufkens, D. J.; Snoeck, T. L.; Lever, A. B. P. *Inorg. Chem.* **1988**, *27*, 953. (d) Lever, A. B. P.; Auburn, P. R.; Dodsworth, E. S.; Haga, M.; Liu, W.; Melnik, M.; Nevin, W. A. *J. Am. Chem. Soc.* **1988**, *110*, 8076. (e) Dodsworth, E. S.; Lever, A. B. P. *Chem. Phys. Lett.* **1990**, *172*, 151. (f) Masui, H.; Lever, A. B. P.; Auburn, P. R. *Inorg. Chem.* **1991**, *30*, 2402. (g) Auburn, P. R.; Dodsworth, E. S.; Haga, M.; Liu, W.; Nevin, W. A.; Lever, A. B. P. *Inorg. Chem.* **1991**, *31*, 3502. (h) Tse, Y.-H.; Auburn, P. R.; Lever, A. B. P. *Can. J. Chem.* **1992**, *70*, 1849. (i) Lever, A. B. P.; Masui, H.; Metcalfe, R. A.; Stufkens, D. J.; Dodsworth, E. S.; Auburn, P. R. *Coord. Chem. Rev.* **1993**, *125*, 317.

(2) (a) DelMedico, A.; Auburn, P. R.; Dodsworth; E. S.; Lever, A. B. P.; Pietro, W. J. *Inorg. Chem.* **1994**, *33*, 1583. (b) DelMedico, A.; Fielder, S. S.; Lever, A. B. P.; Pietro, W. J. *Inorg. Chem.* **1995**, *34*, 1507. (c) DelMedico, A.; Pietro, W. J.; Lever, A. B. P. *Inorg. Chim. Acta* **1998**, *281*, 126.

10.1021/ic035370d CCC: $27.50
Published on Web 03/18/2004

structure. For example, when the Ru^{II}−(*o*-Cat) fragment (in these or related complexes) is oxidized by one electron, this species may be described in several ways, all isoelectronic and differing *only* in charge distribution. Two localized (ionic) descriptions of this are possible, Ru^{III}-(*o*-Cat), where the unpaired electron resides on the metal, or Ru^{II}-(*o*-Sq), where it resides on the ligand.[1a,d,g,4h,6] It may also be described as a mixed system with an unpaired electron in an orbital which has significant contributions from both the metal and the ligand. In highly covalent systems one or other of the formal descriptions may be closer to reality and spectroscopic methods may point to this, but in some systems spectroscopic data are ambiguous and the real situation may be so close to halfway between the two descriptions that neither is useful and we must describe it as highly mixed, or highly covalent. By contrast, a number of first row transition metal dioxolene complexes, in which different charge distributions are possible, show the phenomenon of valence tautomerism or bistability. For these complexes, of cobalt, manganese, and copper, the charge distributions remain localized, and intermolecular electron transfer may occur with change of temperature or solvent, etc.[10]

Scheme 1

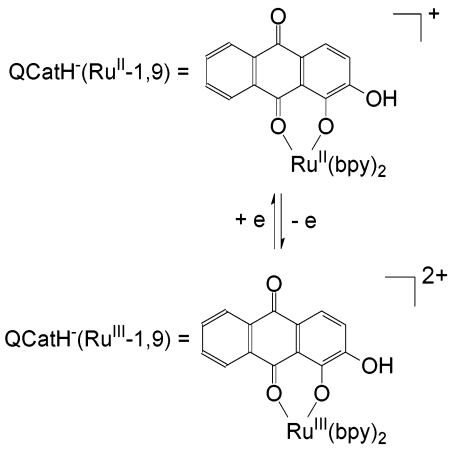

The anionic alizarinate is also an ambidentate ligand, and we have previously characterized complexes containing the $[Ru(bpy)_2]^{2+}$ fragment coordinated to both the 1,9- and 1,2-positions of alizarinate(2−), as well as a method of interconverting (switching) the two isomers.[2a,c] Recent work by Churchill and co-workers[11] also shows that alizarinate may bind ruthenium in either the 1,2- or 1,9-position (they report a crystal structure of a 1,9-coordinated complex), although linkage isomers are not observed.

The related protonated 1,9-species and the corresponding complex of 1-hydroxyanthraquinone were also characterized previously.[2a,c] Here, we report further characterization of members of the redox series derived from the protonated 1,9-coordinated complex and the 1,2-coordinated complex (Schemes 1 and 2, respectively). Spectroelectrochemistry, EPR spectroscopy of odd-electron species, and MO calculations for all species, including the 1-hydroxyanthraquinone analogue, are included.

To understand the coordination of ruthenium−dioxolene complexes, such as those of alizarin, it is critical to examine the extent of delocalization or covalency. This can be a difficult task, particularly for highly coupled metal−dioxolene centers. Structural characterization at times fails to provide an unambiguous assignment of charge distribution.[1b,4h,k,l] For several years this group has been addressing the problem of ambiguity in the electronic structure of ruthenium metal complexes of noninnocent ligands[1−3] and metal−ligand orbital mixing (covalency of the metal−ligand bond).[12]

(3) (a) Auburn, P. R.; Lever, A. B. P. *Inorg. Chem.* **1990**, *29*, 2551. (b) Masui, M.; Lever, A. B. P.; Dodsworth, E. S. *Inorg. Chem.* **1993**, *32*, 258. (c) Metcalfe, R. A.; Dodsworth, E. S.; Lever, A. B. P.; Pietro, W. J.; Stufkens, D. J. *Inorg. Chem.* **1993**, *32*, 3581. (d) Hartl, F.; Snoeck, T. L.; Stufkens, D. J.; Lever, A. B. P. *Inorg. Chem.* **1995**, *34*, 3887. (e) da Cunha, C. J.; Fielder, S. S.; Stynes, D. V.; Masui, H.; Auburn, P. R.; Lever, A. B. P. *Inorg. Chim. Acta* **1996**, *242*, 293. (f) Metcalfe, R. A.; Dodsworth, E. S.; Fielder, S. S.; Stufkens, D. J.; Lever, A. B. P.; Pietro, W. J. *Inorg. Chem.* **1996**, *35*, 7741. (g) Metcalfe, R. A.; Lever, A. B. P. *Inorg. Chem.* **1997**, *36*, 4762. (h) Metcalfe, R. A.; Vasconcellos, L. C. G.; Mirza, H.; Franco, D. W.; Lever, A. B. P. *J. Chem. Soc., Dalton Trans.* **1999**, 2653. (i) da Cunha, C. J.; Dodsworth, E. S.; Monteiro, M. A.; Lever, A. B. P. *Inorg. Chem.* **1999**, *38*, 5399. (j) Ebadi, M.; Lever, A. B. P. *Inorg. Chem.* **1999**, *38*, 476. (k) Masui, M.; Freda, A. L.; Zerner, M. C.; Lever, A. B. P. *Inorg. Chem.* **2000**, *39*, 141. (l) da Silva, R. S.; Gorelsky, S. I.; Dodsworth, E. S.; Tfouni, E.; Lever, A. B. P. *J. Chem. Soc., Dalton Trans.* **2000**, 4078. (m) Lever, A. B. P.; Gorelsky, S. I. *Coord. Chem. Rev.* **2000**, *208*, 153.

(4) (a) Balch, A. L.; Sohn, Y. S. *J. Organomet. Chem.* **1971**, *30*, C31. (b) Balch, A. L. *J. Am. Chem. Soc.* **1973**, *95*, 2723. (c) Girgis, A. Y.; Sohn, Y. S.; Balch, A, L. *Inorg. Chem.* **1975**, *14*, 2327. (d) Giovannitti, B.; Gandolfi, O.; Ghedini, M.; Dolcetti, G. *J. Organomet. Chem.* **1977**, *129*, 207. (e) Pell, S. D.; Salmonsen, R. B.; Abelleira, A.; Clarke, M. J. *Inorg. Chem.* **1984**, *23*, 387. (f) Connelly, N. G.; Manners, I.; Protheroe, J. R. C.; Whiteley, M. W. *J. Chem. Soc. Dalton Trans.* **1984**, 2713. (g) Griffith, W. P.; Pumphrey, C. A.; Rainey, T.-A. *J. Chem. Soc., Dalton Trans.* **1986**, 1125. (h) Boone, S. R.; Pierpont, C. G. *Inorg. Chem.* **1987**, *26*, 1769. (i) Ernst, S.; Hänel, P.; Jordanov, J.; Kaim, W.; Kasack, V.; Roth, E. *J. Am. Chem. Soc.* **1989**, *111*, 1733. (j) Schwederski, B.; Kasack, V.; Kaim, W.; Roth, E.; Jordanov, J. *Angew. Chem., Int. Ed. Engl.* **1990**, *29*, 78. (k) Bhattacharya, S.; Boone, S. R.; Fox, G. A.; Pierpont, C. G. *J. Am. Chem. Soc.* **1990**, *112*, 1088. (l) Boone, S. R.; Pierpont, C. G. *Polyhedron* **1990**, *9*, 2267. (m) Bhattacharya, S.; Pierpont, C. G. *Inorg. Chem.* **1991**, *30*, 1511. (n) Bag, N.; Oramanik, A.; Lahiri, G. K.; Chakravorty, A. *Inorg. Chem.* **1992**, *31*, 40. (o) Bag, N.; Lahiri, G. K.; Basu, P.; Chakravorty, A. *J. Chem. Soc., Dalton Trans.* **1992**, 113. (p) Howard, C. A.; Ward, M. D. *Angew. Chem., Int. Ed. Engl.* **1992**, *31*, 1028. (q) Bohle, D. S.; Christensen, A. N.; Goodson, P. A. *Inorg. Chem.* **1993**, *32*, 4173. (r) Waldhör, E.; Schwederski, B.; Kaim, W. *J. Chem. Soc., Perkin Trans. 2* **1993**, 2109. (s) Bhattacharya, S. *Polyhedron* **1994**, *13*, 451. (t) Bhattacharya, S.; Pierpont, C. G. *Inorg. Chem.* **1994**, *33*, 6038. (u) Joulié, L. F.; Schatz, E.; Ward, M. D.; Weber, F.; Yellowlees, L. J. *J. Chem. Soc., Dalton Trans.* **1994**, 799. (v) Ward, M. D. *Inorg. Chem.* **1996**, *35*, 1712. (w) Barthram, A. M.; Cleary, R. L.; Kowallick, R.; Ward, M. D. *J. Chem. Soc., Chem. Commun.* **1998**, 2695. (x) Shukla, A. D.; Whittle, B.; Bajaj, H. C.; Das, A.; Ward, M. D. *Inorg. Chim. Acta* **1999**, *285*, 89. (y) Barthram, A. M.; Ward, M. D. *New J. Chem.* **2000**, *24*, 501.

(5) (a) Pierpont, C. G.; Buchanan, R. M. *Coord. Chem. Rev.* **1981**, *38*, 45. (b) Kabachnik, M. I.; Bubov, N. N.; Solodnikov, S. P.; Prokof'ev, A. I. *Usp. Khim.* **1984**, *53*, 487; *Russ. Chem. Rev.* **1984**, *53*, 288. (c) Pierpont, C. G. *Prog. Inorg. Chem.* **1994**, *41*, 331.

(6) Vlček, A., Jr. *Comments Inorg. Chem.* **1994**, *16*, 207.

(7) (a) Merrell, P. H. *Inorg. Chim. Acta* **1979**, *32*, 99. (b) Dei, A.; Gatteschi, D.; Pardi, L. *Inorg. Chem.* **1990**, *29*, 1442. (c) Sadler, G. G.; Gordon, N. R. *Inorg. Chim. Acta* **1991**, *180*, 271. (d) Bruni, S.; Cariati, F.; Dei, A.; Gatteschi, D. *Inorg. Chim. Acta* **1991**, *186*, 157. (e) Gooden, V. M.; Cai, H. Q.; Dasgupta, T. P.; Gordon, N. R.; Hughes, L. J.; Sadler, G. G. *Inorg. Chim. Acta* **1997**, *255*, 105.

(8) (a) *The Chemistry of the Quinonoid Compounds*; Patai, S., Ed.; Wiley: New York, 1974; Vol. 1. (b) Stallings, M. D.; Morrison, M. M.; Sawyer, D. T. *Inorg. Chem.* **1981**, *20*, 2655.

(9) Vlcek, A. A. *Coord. Chem. Rev.* **1982**, *43*, 39.

(10) Pierpont, C. G. *Coord. Chem. Rev.* **2001**, *216/217*, 99.

(11) Churchill, M. R.; Keil, K. M.; Bright, F. V.; Pandey, S.; Baker, G. A.; Keister, J. B. *Inorg. Chem.* **2000**, *39*, 5807.

Scheme 2

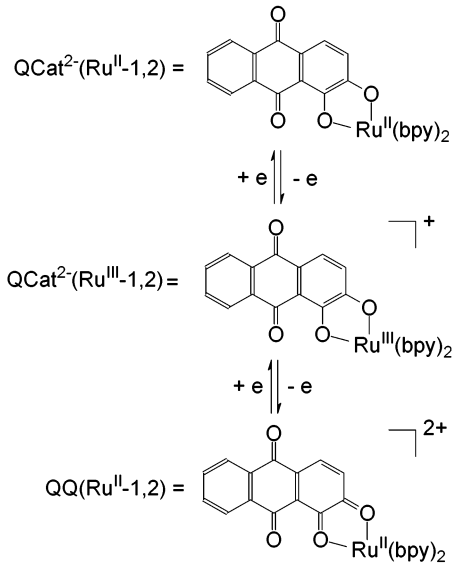

INDO semiempirical molecular orbital calculations, using the ZINDO program,[13] are used here to elucidate the extent of delocalization and to calculate electronic spectra and are found to give results reasonably consistent with experimental data. The ZINDO/S method has been used recently for a variety of ruthenium complexes.[14] We have recently demonstrated that the INDO method using the ZINDO code provides results quite similar to density functional theory (DFT) calculations, using B3LYP, on the same molecules;[14l,o] thus, for larger molecules, where time and computer constraints render DFT calculations inefficient, ZINDO is particularly useful. On the basis of our calculations, we have assigned the visible region spectra of all the complexes reported here, despite the complexity of the spectra due to the multiple chromophores present in the complexes.

Abbreviations

As in previous publications,[2] alizarin is abbreviated here as $QCatH_2$; Q identifies the 9,10-dioxo unit and $CatH_2$ identifies the 1,2-catechol unit. Similarly, $QCatH^-$ and $QCat^{2-}$ correspond to the 1,2-catechol anion and dianion, respectively, and the fully oxidized form is QQ. The term alizarinate is also used to refer to either of the anions (and occasionally to QQ as well) unless one or other is specified. The related 1-hydroxy-9,10-anthraquinone anion is abbreviated as QO^-. The abbreviations used for the complexes include the formal oxidation state of the ruthenium and its coordination site: for example, (Ru^{II}-1,9) indicates that the ruthenium(II)−bis(bipyridine) fragment is coordinated to the 1,9-site.

Experimental Section

Chemicals. All solvents and reagents used were reagent grade or better and were used as purchased except where otherwise stated. All solid compounds were stored in a desiccator in the dark.

Physical Methods. Physical data were recorded on instrumentation as follows: electronic spectra, Varian CARY 2400; and electron paramagnetic resonance (EPR) spectra, Varian model E-4. Controlled potential electrolyses were carried out at a Pt working electrode using an OTTLE cell slightly modified from the design published by Krejcik.[15]

Preliminary resonance Raman spectra were obtained by Dr. B. Lenain at EG&G Company, using a Dilor XY Raman spectrometer. Dichloromethane solutions of the complexes were exposed to an argon laser with the power at 10 mW, and a spectral slit width of 16.91 cm^{-1} for $QCat^{2-}$(Ru^{II}-1,2), and 20.29 cm^{-1} for both $QCatH^-$-(Ru^{II}-1,9) and QO^-(Ru^{II}-1,9).

Theoretical Methods. Optimized geometric structures were obtained using the modified INDO/1 method[13,16] (ZINDO/1) using UNIX developmental code provided by the late Michael Zerner. The ruthenium bases of Krogh-Jespersen[17] were used but with Ru, $\beta(4d) = -18$ eV.

Electronic spectroscopic calculations were performed using the modified INDO/S method[18] (ZINDO/S) using code obtained from Jeff Reimers (Sydney, Australia). This code used RHF and ROHF methods for closed and open shell species, respectively. Coupling parameters were $k_{p\sigma} = 1.267$ and $k_{p\pi} = 0.585$. Electronic spectra were calculated at the single excitation configuration interaction (CIS) level with matrix size 20 × 20 (800 configurations) for closed shell systems and CIS level with matrix size 16 × 16 (512 configurations) for open shell systems ($QCat^{2-}$(Ru^{III}-1,2) and $QCatH^-$(Ru^{III}-1,9)). Percentage compositions of orbitals were calculated from the ZINDO/S data using the AOMIX program.[19] Pictures of orbitals in the closed shell species were obtained by running the same structures on the Hyperchem program (v.5.01

(12) (a) Gorelsky, S. I.; Dodsworth, E. S.; Lever, A. B. P.; Vlcek, A. A. *Coord. Chem. Rev.* **1998**, *174*, 469. (b) Lever, A. B. P. *Can. J. Anal. Sci. Spectrosc.* **1997**, *42*, 24.

(13) Zerner, M. C. *ZINDO program*, version 98.1; Quantum Theory Project, University of Florida: Gainesville, FL.

(14) (a) Bezerra, C. W. B.; da Silva, S. C.; Gambardella, M. T. P.; Santos, R. H. A.; Plicas, L. M. A.; Tfouni, E.; Franco, D. W. *Inorg. Chem.* **1999**, *38*, 5660. (b) Marcaccio, M.; Paolucci, F.; Paradisi, C.; Roffia, S.; Fontanesi, C.; Yellowlees, L. J.; Serroni, S.; Campagna, S.; Denti, G.; Balzani, V. *J. Am. Chem. Soc.* **1999**, *121*, 10081. (c) Ait-Haddou, H.; Bejan, E.; Dran, J.-C.; Balavoine, G. G. A.; Berruyer-Penaud, F.; Bonazzola, L.; Smaoui-Chaabouni, H.; Amouyal, E. *J. Chem. Soc., Dalton Trans.* **1999**, 3095. (d) Constantino, V. R. L.; Toma, H. E.; de Oliveira, L. F. C.; Rein, F. N.; Rocha, R. C.; de Oliveira Silva, D. *J. Chem. Soc., Dalton Trans.* **1999**, 1735. (e) Streiff, J. H.; Edwards, W. D.; McHale, J. L. *Chem. Phys. Lett.* **1999**, *312*, 369. (f) Da Silva, S. C.; Franco, D. W. *Spectrochim. Acta* **1999**, *55A*, 1515. (g) Nazeeruddin, M. K.; Zakeeruddin, S. M.; Humphry-Baker, R.; Gorelsky, S. I.; Lever, A. B. P.; Graetzel, M. Coord. Chem Rev. **2000**, *208*, 213. (h) Rogachevsky, I. V.; Baranovski, V. I. *Spectrochim. Acta* **2000**, *56A*, 2699. (i) Toma. H. E.; Serrasqueiro, R. M.; Rocha, R. C.; Demets, G. J. F.; Winnischofer, H.; Araki, K.; Ribeiro, P. E. A.; Donnici, C. L. *J. Photochem. Photobiol., A* **2000**, *135*, 185. (j) Bagatin, I. A.; Toma, H. E. *Transition Met. Chem.* **2000**, *25*, 686. (k) Gorelsky, S. I.; da Silva, S. C.; Lever, A. B. P.; Franco, D. W. *Inorg. Chim. Acta* **2000**, *300*−*302*, 698. (l) Gorelsky, S. I.; Lever, A. B. P. *J. Organomet. Chem.* **2001**, *635*, 187. (m) Coe, B. J.; Harris, J. A.; Brunschwig, B. S. *J. Phys. Chem. A* **2002**, *106*, 897. (n) Renouard, T.; Fallahpour, R. A.; Nazeeruddin, M. K.; Humphry-Baker, R.; Gorelsky, S. I.; Lever, A. B. P.; Graetzel, M. *Inorg. Chem.* **2002**, *41*, 367. (o) Gorelsky, S. I.; Lever, A. B. P.; Ebadi, M. *Coord. Chem. Rev.* **2002**, *230*, 97.

(15) (a) Krejcik, M.; Danek, M.; Hartl, F. *J. Electroanal. Chem.* **1991**, *317*, 179. (b) Tse, Y.-H. Ph.D. Thesis, York University, 1994.

(16) Anderson, W. P.; Cundari, T. R.; Zerner, M. C. *Int. J. Quantum Chem.* **1991**, *39*, 31.

(17) Krogh-Jespersen, K.; Westbrook, J. D.; Potenza, J. A.; Schugar, H. J. *J. Am. Chem. Soc.* **1987**, *109*, 7025.

(18) (a) Ridley, J.; Zerner, M. C. *Theor. Chim. Acta* **1973**, *32*, 111. (b) Ridley, J.; Zerner, M. C. *Theor. Chim. Acta* **1976**, *42*, 223. (c) Zerner, M. C.; Loew, G. H.; Kirchner, R. F.; Mueller-Westerhoff, U. T. *J. Am. Chem. Soc.* **1980**, *102*, 589. (d) Anderson, W. P.; Edwards, W. D.; Zerner, M. C. *Inorg. Chem.* **1986**, *25*, 2728.

(19) Gorelsky, S. I. *AOMix program and SWizard program*, revision 1; York University: North York, ON, Canada, 2001. The programs are available at http://www.obbligato.com/software/.

and v.6.0, Hypercube, Inc., FL); percentage compositions and energies similar (generally to within 0.01 eV) to those from the Reimers calculation were obtained, indicating that the orbitals are essentially identical using either the Hyperchem program or the Reimers code. The default atomic parameters in the Hyperchem program differ slightly from those used by Reimers; hence, we employ Reimers' parameters in the Hyperchem program. Calculated spectra, assuming a constant half bandwidth of 3000 cm^{-1}, were displayed visually using the SWizard program[19] which sums the calculated oscillator strengths. Calculated intensities are divided by two. All calculated bands are included in the figures, whereas only the more intense ones are listed in the tables.

Preparation of Complexes. $QCat^{2-}(Ru^{II}$-1,2) (blue) was prepared according to the literature.[2a] The RR spectrum in CH_2Cl_2, excited at 514.5 nm, shows resonance enhanced bands at 1585, 1543, 1475, 1436, 1311, 1253, 1165, and 1016 cm^{-1}.

$QCat^{2-}(Ru^{III}$-1,2) (green) was prepared according to the literature.[2c]

$QQ(Ru^{II}$-1,2) (bright blue) was generated from $QCat^{2-}(Ru^{II}$-1,2) by controlled-potential oxidation at 1.0 (or 1.1 or 1.2) V versus AgCl/Ag in CH_2Cl_2 containing 0.1 M tetra-*tert*-butylammonium hexafluorophosphate ($TBAPF_6$).

$QCatH^{-}(Ru^{II}$-1,9) (purple) was prepared according to the literature.[2a] The RR spectrum in CH_2Cl_2, excited at 514.5 nm, shows resonance enhanced bands at 1597, 1551, 1540, 1512, 1478, 1451, 1315, 1265, 1167, and 1022 cm^{-1}.

$QCat^{2-}(Ru^{II}$-1,9) (dark purple) was prepared *in situ* according to the literature.[2a]

$QCatH^{-}(Ru^{III}$-1,9) (orange) was generated *in situ* by adding $NOBF_4$ to $QCatH^{-}(Ru^{II}$-1,9) in acetonitrile at −23 °C, or by controlled potential electrolysis at room temperature. Addition of trifluoroacetic acid to this species in CH_3CN (at −23 °C) resulted in no significant change in the spectrum. Orange solutions of $QCatH^{-}(Ru^{III}$-1,9) slowly decompose to give a yellow species. As the decomposition proceeds, bands at 10600 and 21400 cm^{-1} in the electronic spectrum decrease in absorbance. This decomposition occurs under a variety of conditions: using chemical or electrochemical oxidation, in CH_3CN or CH_2Cl_2 and under an atmosphere of N_2 or of air. However, at −23 °C the reaction slows to a negligible rate; the electronic spectrum of $QCatH^{-}(Ru^{III}$-1,9) in CH_3CN remains unchanged after 30 min at this temperature, and there is little change after 1 h.

$QO^{-}(Ru^{II}$-1,9) (purple) was prepared according to the literature.[2a] The RR spectrum in CH_2Cl_2, excited at 514.5 nm, shows resonance enhanced bands at 1657, 1594, 1551, 1531, 1500, 1474, 1457, 1424, 1313, 1264, 1232, 1167, 1035, and 1021 cm^{-1}.

Attempted Synthesis of $QCat^{2-}(Ru^{III}$-1,9). All attempts to generate $QCat^{2-}(Ru^{III}$-1,9), *in situ*, failed. This seems to be due to the instability of the protonated species and the limited choices of nonreducing and volatile bases. Reactions were performed in CH_3CN and were carried out in dry conditions. We were unable to find a nonreducing base which would reversibly deprotonate the protonated species.

Results and Discussion

We have reported that bis(bipyridine)ruthenium(II), $[Ru(bpy)_2]^{2+}$, can be coordinated to alizarinate by either the 1,2- or 1,9-coordination site,[2a,c] and that the two complexes can be interconverted by a combination of proton-transfer and thermal methods.[2a] We also previously reported the preparation of the first oxidation product of $QCat^{2-}(Ru^{II}$-1,2).[2c] We have now extended the redox series of both the 1,9-coordinated complex (Scheme 1) and the 1,2-coordinated complex (Scheme 2) by preparing $QCatH^{-}(Ru^{III}$-1,9) and $QQ(Ru^{II}$-1,2) in solution. $QQ(Ru^{II}$-1,2) has been characterized by its electronic spectrum, which is very similar to that of other ruthenium quinone complexes[1a,c,f] and is in good agreement with the calculated spectrum (below). $QCatH^{-}(Ru^{III}$-1,9) has been characterized by EPR and electronic spectroscopy. This latter species is expected to contain an acidic proton, but we were unable to remove it without simultaneously re-reducing the complex. However, addition of acid to the solution caused no change in the electronic spectrum, evidence that the proton is still present. The solution is also somewhat unstable in solution at room temperature, but the decomposition is sufficiently slow at −23 °C that spectroscopic data could be obtained.

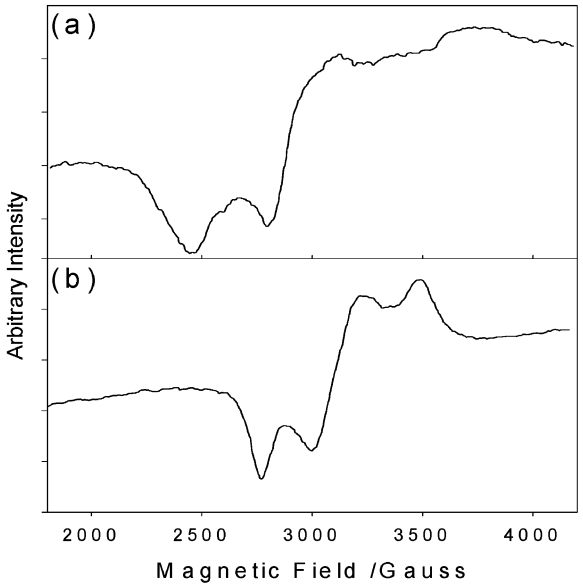

Figure 1. EPR spectra of complexes at ca. 77 K: (a) $QCatH^{-}(Ru^{III}$-1,9) in frozen DCM; (b) $QCat^{2-}(Ru^{III}$-1,2) in 4:1 EtOH/MeOH glass.

We discuss here results of geometry optimizations, and calculations of molecular orbital energies and electronic spectra of all the above species. Results are compared with data from spectroscopic techniques.

Electron Paramagnetic Resonance Spectroscopy. $QCat^{2-}$-$(Ru^{III}$-1,9). For EPR of $QCatH^{-}(Ru^{III}$-1,9), the best results were obtained by an *in situ* oxidation of $QCatH^{-}(Ru^{II}$-1,9) with an excess of $AgPF_6$. As shown in Figure 1, a frozen dichloromethane solution at 77 K exhibits an anisotropic signal with three distinct g values: $g = 2.61$, 2.18 (pp = 225 G), 1.72 (pp is the peak to peak separation). At room temperature the sample is EPR-silent, typical of a Ru^{III} species.[20] The anisotropic signal and large peak to peak separation at 77 K are also normally regarded as characteristic of a low spin, d^5, ruthenium(III) complex,[20] i.e., formally Ru^{III}−(*o*-Cat). This is consistent with the previously reported electrochemical data in which complexes $QCatH^{-}(Ru^{III}$-1,9) and $QO^{-}(Ru^{II}$-1,9), show reversible couples assigned as

(20) (a) Bleaney, B.; Stevens, K. W. H. *Rep. Prog. Phys.* **1953**, *16*, 108. (b) Gordy, W. In *Theory and Applications of Electron Spin Resonance*; John Wiley and Sons Inc.: New York, 1980. (c) Rieger, P. H. *Coord. Chem. Rev.* **1994**, *135/136*, 203.

Table 1. Calculated C−O and Metal−Ligand Bond Lengths (Å)

species	M−N trans N	M−N trans O	M−O1	M−O2/O9	C−O1	C−O2	C−O9	C−O10
$QCatH_2$					1.33	1.35	1.27	1.26
$QCatH^-$					1.32	1.32	1.26	1.26
QOH					1.33		1.27	1.26
QO^-					1.28		1.27	1.26
$QCatH^-(Ru^{II}$-1,9)	2.05	2.06	1.96	1.96	1.33[a]	1.34[a]	1.28	1.26
$QCat^{2-}(Ru^{II}$-1,9)	2.05	2.07	1.93	1.94	1.31	1.27	1.3	1.27
$QCatH^-(Ru^{III}$-1,9)	2.05	2.05[b], 2.06[b]	1.98	1.97	1.32[a]	1.31[a]	1.28	1.3
$QO^-(Ru^{II}$-1,9)	2.05	2.06, 2.07(O1[c])	1.94	1.95	1.31		1.29	1.26
$QCat^{2-}(Ru^{II}$-1,2)	2.05	2.06[b], 2.07[b]	1.96	1.96	1.33	1.33	1.26	1.26
$QCat^{2-}(Ru^{III}$-1,2)	2.05	2.05, 2.06(O2[c])	1.97	1.97	1.33	1.32	1.26	1.26
$QQ(Ru^{II}$-1,2)	2.05	2.04[b], 2.05[b]	1.98	1.99	1.28	1.28	1.26	1.26

[a] Note that the OH hydrogen of the $CatH^-$ species appears to be strongly H-bonded to O1. [b] These differences are of the order of 0.002−0.003 Å but appear larger due to rounding. [c] Longer Ru−N is trans to O1or O2 as specified.

$Ru^{III/II}$, at approximately the same potential.[2a] INDO/S results using the ROHF method (discussed below) are also consistent with Ru^{III}.

$QCat^{2-}(Ru^{III}$-1,2). $QCat^{2-}(Ru^{III}$-1,2), while EPR-silent at room temperature, shows an anisotropic EPR spectrum at 77 K (4:1 EtOH/MeOH glass), with *g* values 2.30, 2.05 (pp = 225), and 1.83 (Figure 1), Again this is consistent with INDO/S results (see below), and with IR data.[2c] The *g* values are similar to those of $[Ru_2(bpy)_4(tetrox)]^{3+}$ (where tetrox is 1,4,5,8-tetraoxonaphthalene) which Dei and co-workers interpret as being a class III mixed-valence, $Ru^{II}-Ru^{III}$, species, with some delocalization of the unpaired electron onto the bridging ligand.[7b]

In a previous paper,[2a] we suggested that, in accord with other ruthenium dioxolene complexes,[1a,f,4r,v] this species was a ligand-based radical because it gave rise to a broad EPR signal with a *g* value of 2.02 in frozen dichloromethane at 77 K. A variety of other media (1:1 CH_2Cl_2/toluene mixture or 1:1 CH_3CN/toluene) gave similar results. Thus, it is possible that the electronic distribution may be somewhat solvent-dependent, though the electronic spectrum shows little evidence of variation between solvents. $QCat^{2-}(Ru^{III}$-1,2) exhibits a fairly intense, narrow, low energy electronic transition at 10600 cm^{-1} (see below) which is similar to that observed at 11250 cm^{-1} in the related species $[Ru^{II}(bpy)_2$-sq$]^+$ and $[Ru^{II}(bpy)_2$dtbsq$]^+$ (sq = *o*-semiquinonate, dtbsq = 3,5-di-*tert*-butylsemiquinonate), which certainly contain ligand-based radicals.[1a,f] However, we note that the analogous osmium complex containing dtbsq has an EPR spectrum which is characteristic of Os^{III}, while having an electronic spectrum similar to the analogous Ru^{II} complexes.[21]

Structural Calculations

Calculations were carried out on the free ligands and their monoanions using the ZINDO/1[13] program. In the initial input structures (prior to geometry optimization), protons attached to C1 (and C2) were oriented so as to maximize intramolecular H-bonding with O9 (and O1), respectively. The ligand structures tend to optimize with rather long C═O distances, and constraining these bond lengths to typical C═O distances for quinones improves the fit between calculated and observed electronic spectra. However, to be consistent with the calculations for the complexes, we report the data for unconstrained structures here. The X-ray structure of the alizarin ligand[22] has C—O distances that vary for the different molecules in the unit cell, and appear to be strongly influenced by intermolecular hydrogen bonding. Two of the molecules in the unit cell have C—O distances that suggest an internal proton transfer, from O1 to O9, has occurred.

We were unable to optimize the structure of the experimentally unavailable deprotonated complex, $QCat^{2-}(Ru^{III}$-1,9), in order to compare with data obtained for $QCatH^-$-$(Ru^{III}$-1,9).

INDO/1 gives very reasonable structures for the basic carbon−nitrogen organic frameworks of the ligands (see Supporting Information),[23] but in order to obtain metal−ligand bond lengths close to literature values from X-ray data for similar Ru complexes,[1b,4h,k,l,11,24−27] it was necessary to decrease the β(4d) value. The best results were obtained with β(4d) = −18 eV. This gave Ru−N in a narrow range around 2.06 Å and Ru−O distances of around 1.93−1.98 Å. Metal−ligand distances are given in Table 1. These Ru−O distances are still rather short, especially for Ru^{II} complexes which are expected to be over 2 Å.[4h,11] Larger β(4d) values, such as those used as the default values in the Hyperchem program, give even shorter metal−ligand bond lengths. However, small changes in these bond lengths do not significantly influence the electronic spectra or the conclusions concerning electronic coupling.

The metal−ligand distances obtained with β(4d) = −18 eV are, however, less sensitive to changes in charge and oxidation state, and to the other ligands in the coordination sphere, than expected. For example, although the Ru−N bond lengths are similar for Ru^{II} and Ru^{III}, in *cis*-$Ru(bpy)_2XY$ complexes, Ru−N *trans* to Ru−N is longer than Ru−N *trans* to Ru−(π-donor), as seen in the structure of $[Ru(bpy)_2Cl_2]$.[25b]

(21) Haga, M.; Isobe, K.; Boone, S. R.; Pierpont, C. G. *Inorg. Chem.* **1990**, *29*, 3795.
(22) Guilhem, J. *Bull. Soc. Chim. Fr.* **1967**, 1666.
(23) Allen, F. H.; Kennard, O.; Watson, D. G.; Brammer, L.; Orpen, A. G.; Taylor, R. *J. Chem. Soc., Perkin Trans. 2* **1987**, S1.
(24) (a) Rillema, D. P.; Jones, D. S.; Levy, H. A. *J. Chem Soc., Chem. Commun.* **1979**, 849. (b) Belser, P.; von Zelewsky, A.; Zehnder, M. *Inorg. Chem.* **1981**, *20*, 3098.
(25) (a) Eggleston, D. S.; Goldsby, K. A.; Hodgson, D. J.; Meyer, T. J. *Inorg. Chem.* **1985**, *24*, 4573. (b) Clear, J. M.; Kelly, J. M.; O'Connell, C. M.; Vos, J. G.; Cardin, C. J.; Costa, S. R.; Edwards, A. J. *J. Chem Soc., Chem. Commun.* **1980**, 750.
(26) Carugo, O.; Castellani, C. B.; Djinović, K.; Rizzi, M. *J. Chem. Soc., Dalton Trans.* **1992**, 837.
(27) Chao, G. K.-J.; Sime, R. L.; Sime, R. J. *Acta Crystallogr.* **1973**, *B29*, 2845.

By contrast, INDO/1 structures have either all Ru−N approximately equal, or Ru−N *trans* to N longer than Ru−N *trans* to O, regardless of the charge on the alizarinate ligand. The changes in bond lengths upon oxidation are also very small; Ru−N values vary little, and Ru−O values increase in length (by 0.01 Å) rather than decreasing as we would expect. This latter effect is consistent across the 1,2-coordinated series, with Ru−O distances increasing upon oxidation to 1.98−1.99 Å in QQ(Ru^{II}-1,2). However, there are variations in the C−C distances indicating some change from aromatic to quinonoid structure (in the ring nearest to the Ru), across the 1,2-coordinated series, with change of oxidation state. These changes, which are monotonic, suggest that the ZINDO/1 structure tends toward a Ru^{II}−semiquinone description, rather than a Ru^{III}−catechol, as given by ZINDO/S. That the two programs would give different results is not surprising since they are parametrized for structure and spectra, respectively.

C−O distances in complexes of catechols and their derivatives are generally regarded as being indicative of ligand oxidation state.[5,6,26] In $QCat^{2-}$(Ru^{II}-1,2) and its oxidation products, assuming that the alizarinate retains a localized "QCat" structure, there are expected to be clear differences between the two sets of C−O distances: the coordinated C−O's, which will vary with redox state, and the uncoordinated C═O's of the *p*-quinone fragment, which are expected to remain quinonoid. ZINDO/1 results for the $QCat^{2-}$(Ru^{II}-1,2) series show this pattern (Table 1); the quinonoid C═O values remain at 1.26 Å throughout the series and the catechol fragment (1,2-position) C−O's (1.33 Å) show almost no change when the Ru is oxidized to Ru^{III}, and then decrease to 1.28 Å in QQ(Ru^{II}-1,2). However, 1.26 Å is rather long for a quinone C═O, the expected distance being around 1.22 Å.[11,23] A value of 1.33 Å is on the short side of the catechol C−O range, and 1.28 Å, in QQ(Ru^{II}-1,2), is more typical of a coordinated semiquinonate than of a quinone.

In the 1,9-series, including QO^-(Ru^{II}-1,9), the uncoordinated C═O in the 10-position remains at 1.26−1.27 Å in the Ru^{II} species and is longer, 1.28 Å, in $QCatH^-$(Ru^{III}-1,9). Its coordinated counterpart is 1.28−1.29 Å in $QCatH^-$(Ru^{II}-1,9) and QO^-(Ru^{II}-1,9) and longer, 1.30 Å, in both $QCat^{2-}$-(Ru^{II}-1,9) and, surprisingly, $QCatH^-$(Ru^{III}-1,9). The alizarinate dianion is completely delocalized according to AM1 calculations,[28] so in the absence of solvent, protons, or a coordinated metal, the distinction between single and double C−O bonds is lost. In $QCat^{2-}$(Ru^{II}-1,9) both uncoordinated C−O's are 1.27 Å, and the coordinated ones are 1.30−1.31 Å, suggesting a structure which is no longer "QCat". This and the pattern of long and short C−C distances suggest a diradical canonical form. When this complex is protonated, as in $QCatH^-$(Ru^{II}-1,9), the structure reverts to the "QCat" form with C1−O and C2−O long (1.33−1.34 Å), and C9−O and C10−O short (1.26, 1.28 Å). The QO^- complex is similar, but it appears to have slightly more delocalized Ru−QO^- bonding in the chelate ring, on the basis of the similarity of the two bound (to Ru) C−O distances, 1.29 Å (C9−O) and 1.31 Å (C1−O). $QCatH^-$(Ru^{III}-1,9) is surprisingly different from $QCatH^-$(Ru^{II}-1,9), seeming to be less localized, with long uncoordinated C−O bonds (1.30 Å for C10−O and 1.31 Å for C2−O) as well as a long C1−O distance. The C10−O length is the most surprising because it is expected to be a quinonoid C═O. C9−O is the only C−O bond length in this complex that lies in the normal Sq or Q range. There are crystal structures of 1,9-analogues in the literature with both localized and delocalized bonding within the chelate ring.[11,29] The delocalized structures, though, are seen for symmetric bridging ligands, tetraoxoanthracene and tetraoxonaphthalene, and have C−O lengths of 1.28−1.30 Å, typical of coordinated semiquinones. In calcium aluminum alizarinate[29a] both the 1,2- and 1,9-sites are coordinated to metal atoms. The catechol C−O distances are 1.31 Å, and the quinonoid C═O are approximately 1.23 Å. In Churchill's $RuH(CO)(PPh_3)_2QCatH$, a $QCatH^-$(Ru^{II}-1,9) analogue, the bonding is clearly localized with the C═O lengths being 1.23 and 1.25 Å, and the C−O being 1.31 and 1.35 Å.[11]

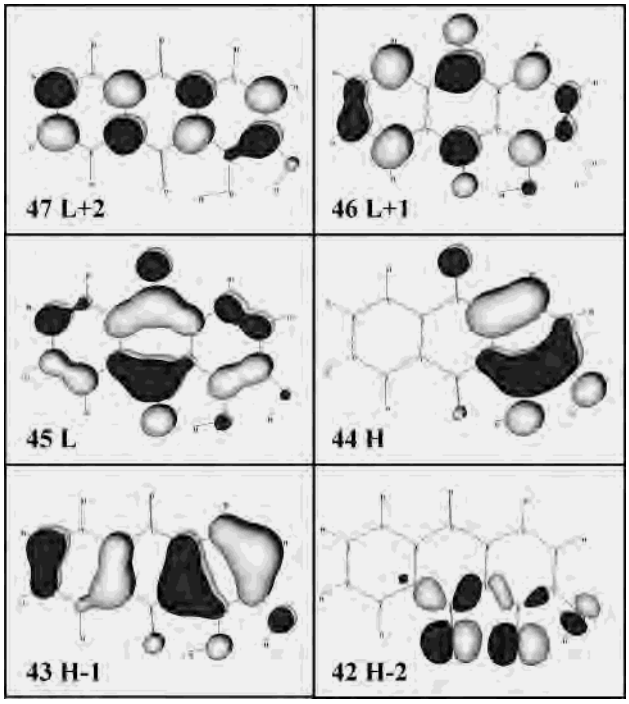

Figure 2. Valence orbitals of alizarin calculated by INDO/S.

Orbitals and Mixing

Free Ligand. Some of the molecular orbitals of the neutral alizarin ligand, $QCatH_2$, are depicted in Figure 2. The orbitals of 1-hydroxyanthraquinone are very similar to those of alizarin. Calculations were also carried out on the anions of both ligands and attempted for the dianion of alizarin, but this failed to give a good structure; the INDO method tends

(28) DelMedico, A.; Lever, A. B. P.; Pietro, W. J. Unpublished observations.

(29) (a) Wunderlich, C.-H.; Bergerhoff, G. *Chem. Ber.* **1994**, *127*, 1185. (b) Heinze, K.; Mann, S.; Huttner, G.; Zsolnai, L. *Chem. Ber.* **1996**, *129*, 1115.

to perform poorly for negatively charged species, particularly those with multiple charges.[30] The orbitals are similar for alizarin and its monoanion, but the HOMO − 1 and HOMO − 2, which are π and σ, respectively, in $QCatH_2$, exchange in relative energies in $QCatH^-$. We refer to ligand orbitals according to the numbering in the neutral, $QCatH_2$, ligand. Thus, 44 is the highest occupied molecular orbital (HOMO) and 45 is the lowest unoccupied molecular orbital (LUMO), and these are π and π^*, respectively. For 1-hydroxyanthraquinone, the HOMO and LUMO are 41 and 42, respectively.

To facilitate comparison with other systems it is helpful to consider the alizarin orbitals as in- and out-of-phase combinations of the MOs of *o*-catechol and naphthoquinone. Due to the larger number of atoms in the π system, there are more π orbitals close in energy to the metal valence levels than there are in catechol. In catechol itself (C_{2v} symmetry, molecule in *xz* plane), the π and π^* orbitals are either a_2 or b_2 in symmetry, with both the HOMO and the LUMO being b_2, i.e., coefficients on oxygen are in phase.[31] The next highest filled π level is a_2 in symmetry, and this forms the π-donor HOMO of *o*-quinone when catechol is oxidized. The b_2 catechol HOMO then becomes the quinone LUMO.[31]

The highest occupied π level of alizarin (44) is delocalized over the whole ligand and has coefficients of the same phase on all three oxygen atoms involved in coordination to ruthenium (O1, O2, and O9). Thus, as far as symmetry is concerned, the interaction of this orbital with the d orbitals is the same for coordination in the 1,2- and 1,9-positions (which may help to facilitate the switch between the two isomers), and it is similar to the interaction of the catechol HOMO with the d orbitals. The second highest π level is alizarin 42 which is also shown in Figure 2.

The alizarin LUMO is also similar to that of catechol from the perspective of a 1,2-coordinated Ru atom, but it is different from the point of view of a metal atom coordinated in the 1,9-position (the coefficients of the two coordinating oxygen atoms are out of phase). Thus, to a 1,2-coordinated Ru, the alizarinate(2−) ligand resembles catecholate, and the two oxidized forms resemble *o*-semiquinonate and *o*-quinone, respectively. For Ru coordinated in the 1,9-position, the chelate ring has six rather than five members, and the interaction with the LUMO must involve a d orbital other than the one which interacts with the HOMO.

The highest energy σ level (43) has electron density on all four oxygen atoms and thus should interact with a Ru atom coordinated in either the 1,2- or the 1,9-position. It has a bonding interaction with the d_{xy} orbital when the ligand is 1,2-coordinated but is nonbonding with respect to 1,9-coordination (see Figure 2).

1,9-Coordinated Complexes. Molecular orbital diagrams for the 1,9-coordinated species, obtained from ZINDO/S calculations, are shown in Figure 3, and the valence orbitals of selected complexes are depicted in Figure 4. The alizarin ligand is assumed to lie in the *xy* plane in all cases. In two of these four complexes, $QCatH^-(Ru^{II}\text{-}1,9)$ and $QO^-(Ru^{II}\text{-}1,9)$, it is convenient to place the axes along the metal−ligand bonds, in which case the usual d orbitals, d_{xz}, d_{yz}, and d_{xy}, form what would be the t_{2g} set in a complex of O_h symmetry. In $QCat^{2-}(Ru^{II}\text{-}1,9)$, the d orbitals are hybridized for more favorable overlap with the ligand; d_{xz} and d_{yz} combine in- and out-of-phase to form dπ and dδ, respectively, i.e., as if the complex had C_{2v} symmetry. This also occurs for the 1,2-coordinated species. Normally when this occurs we would rotate the axes so that the C_2 axis, *z*, lay between the two Ru−O bonds. We have not done that here for the sake of comparison of all the species. For the Ru^{III} species, the hybridization is not simple, but the Ru orbitals are reasonably well described by pseudo-C_{2v} symmetry, i.e., dπ, dδ, and dσ or d_{xy}. The fractional orbital mixing in the frontier orbitals is shown in Table 2. The degree of mixing with the alizarinate ligand is not exceptionally high in any of the (Ru^{II}-1,9) complexes, as was concluded by Gooden et al. for other $[Ru(bpy)_2]^{2+}$ complexes of other dihydroxyanthraquinones.[7e]

Although we focus mainly on interactions between Ru and alizarinate, and use the $[Ru(bpy)_2]^{2+}$ fragment as a spectator,[32] there is mixing of about 11−20% bpy(π) character into each of the filled d levels of the (Ru^{II}-1,9) complexes, and about 7% in the Ru^{III} SOMO. There is little π back-donation to alizarinate π^* levels in these species (5% maximum) and only moderate amounts to bpy (4−8% maximum in the Ru^{II} species). The interaction with bpy is similar to that in other

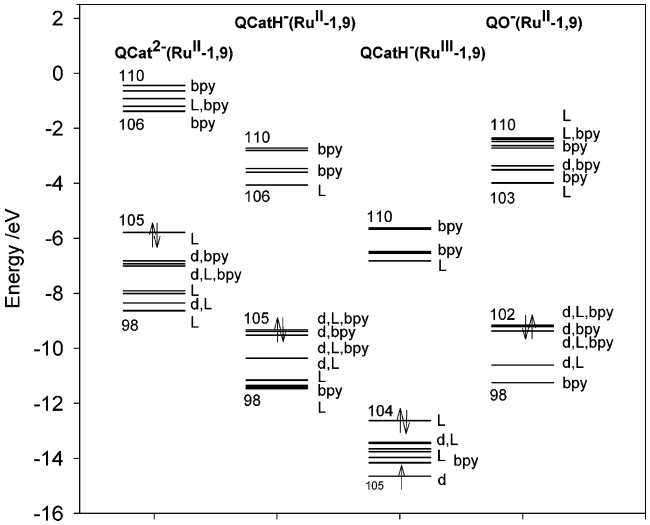

Figure 3. INDO/S molecular orbital energies of 1,9-coordinated alizarin and 1-hydroxyanthraquinone bis(bipyridine)ruthenium complexes. The molecular orbital labels reflect the major contributors to each orbital: bipyridine (bpy), alizarin (L), and/or ruthenium (d). Where there are two or more significant contributions, the orbital listed first is the main contributor. The HOMOs are indicated by arrows representing electron pairs. In the Ru(III) species, the SOMO (marked with a single arrow) is not calculated to be the highest energy orbital; see text.

(30) Zerner, M. C. In *Reviews in Computational Chemistry*; Lipkowitz, K. B., Boyd, D. B., Eds; VCH Publishers, Inc.: New York, 1991, Vol. 2, p 313.

(31) (a) Gordon, D. J.; Fenske, R. F. *Inorg. Chem.* **1982**, *21*, 2907, 2916. (b) Bianchini, C.; Masi, D.; Mealli, C.; Meli, A.; Martini, G.; Laschi, F.; Zanello, P. *Inorg. Chem.* **1987**, *26*, 3683.

(32) Bowden, W. L.; Little, W. F.; Meyer, T. J.; Salmon, D. *J. Am. Chem. Soc.* **1975**, *97*, 6897.

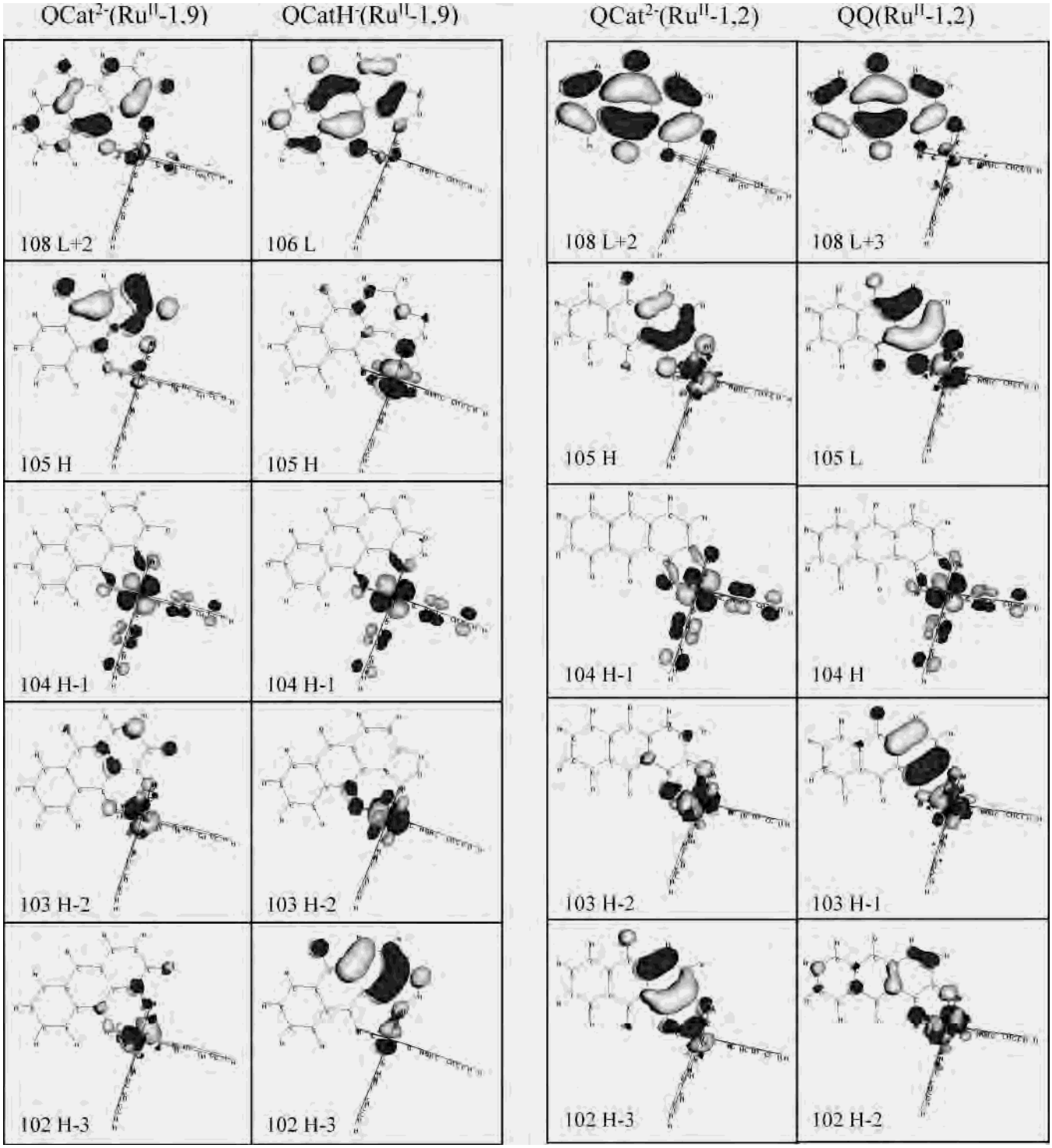

Figure 4. Valence molecular orbitals of selected complexes calculated by INDO/S.

complexes of ruthenium(II) and bipyridine which we have studied.[12a]

$QCatH^{-}(Ru^{II}$-1,9). The Ru(d) orbitals lie above $QCatH^{-}$ HOMO, which forms the HOMO − 3 of the complex. The LUMO of the complex is the $QCatH^{-}$ LUMO which lies significantly lower than the bpy(π_1*) levels (Figure 3), as it does for all the 1,9-species apart from $QCat^{2-}(Ru^{II}$-1,9). Even so, there is very little π-back-bonding to this orbital. Orbitals d_{xz} and d_{yz} have the correct symmetry to combine with alizarinate orbitals of π symmetry, but according to INDO/S, only d_{xz} interacts strongly. It interacts with the free ligand HOMO, orbital 44, binding to the 1-oxygen (Figure 2) resulting in in- and out-of-phase combinations, MOs 102 and 105, respectively (Figures 3 and 4), of which the latter is mainly d. Metal orbital d_{xy} (104, HOMO − 1) is σ in symmetry with respect to $QCatH^{-}$, but neither it nor d_{yz} (HOMO − 2) interacts strongly with the alizarinate(1−) ligand.

$QCat^{2-}(Ru^{II}$-1,9). (See Figures 3 and 4.) Upon deprotonation of the complex, the alizarinate valence levels are raised

Table 2. Fractional Orbital Mixing in the Frontier Orbitals for the 1,9-Coordinated Alizarin Complexes[a,b]

	$QCatH^-(Ru^{II}$-1,9)			$QCat^{2-}(Ru^{II}$-1,9)			$QCatH^-(Ru^{III}$-1,9)				$QO^-(Ru^{II}$-1,9)		
MO	% Ru	% A	% bpy	% Ru	% A	% bpy	% Ru	% A	% bpy	MO	% Ru	% A	% bpy
110	2.3	0.6	97.1	2.7	0.6	96.7	0.7	0.1	99.2	107	2.3	0.8	96.9
109	0.9	0.1	99	1.3	0.2	98.5	0.7	0.1	99.2	106	0.8	0.1	99.1
108	7.4	2.3	90.3	4.8 dδ	82.1	13.1	3.5	1.6	94.9	105	7.8	2.2	90
107	3.6	1	95.4	5.1	13.9	81	1.5	1	97.5	104	3.7	0.8	95.5
106	2.2	94	3.8	4.8	1.2	94	0.6	96.7	2.7	103	2.3 d_{yz}	94.5	3.2
105	***67.0 d_{xz}***	***21.7***	***11.3***	**4.8 dπ**	**94.1**	**1.1**	***86.9 dδ***	***6.3***	***6.8***	102	***66.5 d_{xz}***	***21.9***	***11.6***
104	*72.7 d_{xy}*	*7.8*	*19.5*	*70.1 dσ*	*9.9*	*20*	3.2 dπ	95.7	1.1	101	*72.0 d_{xy}*	*8.1*	*19.9*
103	*73.5 d_{yz}*	*11.3*	*15.2*	*62.3 dπ*	*25.4*	*12.3*	*61.6 dσ*	*18.9*	*19.5*	100	*73.4 d_{yz}*	*11.7*	*14.9*
102	*12.1*	*83.9*	4	*71.9 dδ*	*14.1*	*14*	*52.0 dπ*	*33*	*15*	99	11.1	82.2	6.7
101	0.7	91.7	7.6	1.3	97.6	1.1	6.7	90.9	2.4	98	1	5.4	93.6
100	1.1	7.4	91.5	8.3	88.8	2.9	8.6	87	4.4	97	0.1	90.9	9
99	1	1.4	97.6	0.1	99.8	0.1	0.1	99.8	0.1	96	0.8	6.5	92.7
98	0	99.9	0.1	0.1	99.7	0.2	0.3	2.3	97.4	95	0	100	0

[a] The HOMO (or SOMO) is in bold type; mainly Ru, i.e., the "t_{2g}", orbitals are shown in italics. [b] For the complexes in which there is a strong metal−alizarin π interaction, the d_{xz} and d_{yz} orbitals combine in- and out-of-phase to give orbitals which are labeled dπ and dδ. For consistency, d_{xy} can be labeled dσ in these species.

relative to those of the $[Ru(bpy)_2]^{2+}$ fragment so the lowest $QCat^{2-}$ π* level lies above bpy(π_1*), and the "d" orbitals, which are 60−70% d in character, lie between the two highest $QCat^{2-}$ π levels, separated from both by about 1 eV in energy. As mentioned above, the d_{yz} and d_{xz} orbitals combine in- and out-of-phase, to give a π and a δ combination. dπ interacts with both of the highest lying π levels of the $QCat^{2-}$ ligand (44 and 42) and contributes to the HOMO (which resembles the free ligand HOMO) and HOMO − 2 (mostly d, but whose π component resembles 42 of the ligand) of the complex. dδ interacts with the lowest $QCat^{2-}$ π*, forming orbitals 102 and 108 (HOMO − 3 and LUMO + 2) of the complex. These descriptions are approximate due to the low symmetry; the d component of 108 is not exactly δ. d_{xy} interacts with a $QCat^{2-}$ σ orbital and is the main contributor to the HOMO − 1 of the complex. There is very much less mixing between the d orbitals and the $QCat^{2-}$ valence orbitals in this species than in the isoelectronic $QCat^{2-}(Ru^{II}$-1,2), but there are essentially equal amounts of Ru(d) character in the bpy-based LUMO and LUMO + 1 and the $QCat^{2-}$-based LUMO + 2 (5%). The dδ contribution to the LUMO + 2 is the largest amount of back-bonding to this orbital in any of the complexes discussed here, being significantly more than in the isoelectronic $QCat^{2-}(Ru^{II}$-1,2) species (below). This may be due to the favorable combination of having a doubly negatively charged ligand and having direct overlap between Ru and the quinone functional group, which occurs in the 1,9- but not in the 1,2-complex.

$QCatH^-(Ru^{III}$-1,9). There are many problems associated with calculations involving open shell species.[33] However, we obtain a reasonable match for the electronic spectrum for this complex (see below), which gives us some confidence in the validity of our results. The SOMO is also calculated to have 87% Ru(d) character, in agreement with the EPR spectrum which indicates Ru^{III}, rather than Ru^{II} with the ligand in the semiquinonate oxidation state.

The nature of the valence orbitals is inferred from the Ru(d) coefficients and from the mixing with bpy (which is normally highest for d_{xy} and lowest for dπ). Our inferences are also supported by the calculated transition intensities. Thus, we conclude that the d_{yz} and d_{xz} orbitals combine at least partially, in- and out-of-phase, to give orbitals that approximate to a π and a δ combination. The latter combination is the SOMO. As in the deprotonated species, $QCat^{2-}(Ru^{II}$-1,9), the highest fully occupied level is a ligand π level, (104), with two occupied, mainly d, levels (dπ and d_{xy} or dσ) about 1 eV below it. These two "d" levels have significant $QCat^{2-}$ character, especially the lower one (dπ), which is only 52% Ru. The SOMO is the least mixed of the t_{2g} orbitals and is orbital 105, but with a calculated energy lower than the first eight occupied levels. This observation arises from the way the program treats (separates) the occupied, partially occupied, and unoccupied manifolds.

$QO^-(Ru^{II}$-1,9). This complex is the simplest one discussed here in the sense that the ligand has only one possibility for bidentate coordination (in the 1,9-position) and there is no acidic proton. As in the analogous $QCatH^-(Ru^{II}$-1,9) complex, each d orbital remains relatively pure (around 70% metal character), and the interactions are similar to those in $QCatH^-(Ru^{II}$-1,9). d_{xz} shows the strongest interaction with a ligand orbital, the QO^- HOMO. The orbital ordering and energies are also similar to those in $QCatH^-(Ru^{II}$-1,9) (Figure 3).

1,2-Coordinated Complexes. Orbital energy level diagrams for the redox series of 1,2-coordinated alizarinate complexes, calculated using the ZINDO/S method, are shown in Figure 5, and the fractional orbital mixing in the frontier orbitals is given in Table 3. In these complexes, the d orbitals are hybridized as they would be if the complex had C_{2v} symmetry (see above). dπ overlaps well with the $QCat^{2-}$ HOMO (44), and dδ interacts with the next highest $QCat^{2-}$ π level (42). The $QCat^{2-}(Ru^{III}$-1,2) complex is more complicated due to apparent mixing of σ and π levels in the valence d orbitals.

In most of the 1,2-series, as in the 1,9-series, there is little back-donation to the bpy orbitals; the maximum is 9% d character in a bpy(π_1*) level in $QCat^{2-}(Ru^{II}$-1,2), and there is 5% or less in the other cases. There is little back-donation to the $QCat^{2-}$ LUMO, 45 of the free ligand, (0.1−2% d

(33) Bally, T.; Borden, W. T. In *Reviews in Computational Chemistry;* Lipkowitz, K. B., Boyd, D. B., Eds.; Wiley-VCH Inc.: New York, 1999; Vol. 13, p 1.

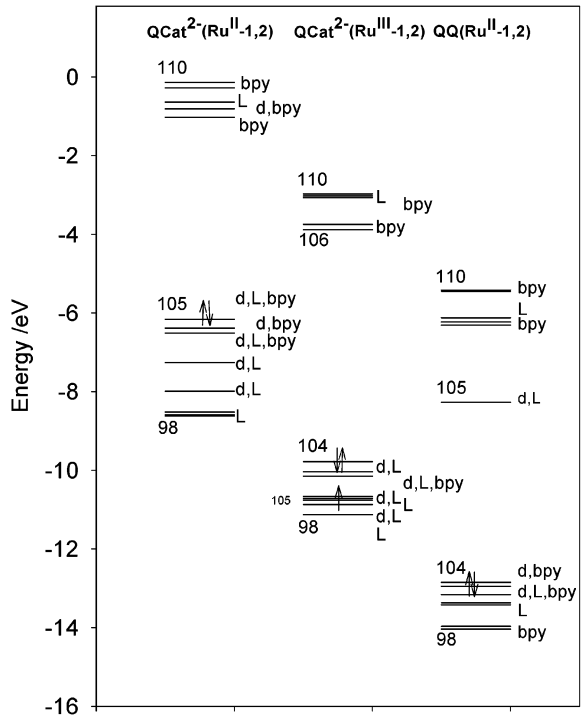

Figure 5. INDO/S molecular orbital energies of 1,2-coordinated alizarin bis(bipyridine)ruthenium complexes. The molecular orbital labels reflect the major contributors to each orbital: bipyridine (bpy), alizarin (L), and/or ruthenium (d). Where there are two or more significant contributions, the orbital listed first is the main contributor. The HOMOs are indicated by arrows representing electron pairs. In the Ru(III) species the SOMO (marked with a single arrow) is not calculated to be the highest energy orbital; see text.

Table 3. Fractional Orbital Mixing in the Frontier Orbitals for the 1,2-Coordinated Alizarin Complexes[a,b]

	$QCat^{2-}(Ru^{II}$-1,2)			$QCat^{2-}(Ru^{III}$-1,2)			$QQ(Ru^{II}$-1,2)		
MO	% Ru	% A	% bpy	% Ru	% A	% bpy	% Ru	% A	% bpy
110	3.6	0.1	96.3	1.6	1.1	97.3	1.1	0.2	98.7
109	0.9	0	99.1	0.1	96.4	3.5	1.6	0.2	98.2
108	0.3	98.4	1.3	0.7	0.8	98.5	2.2	89.4	8.4
107	9.4	0.7	89.9	4.9	0.3	94.8	4	1.9	94.1
106	4.9	1.6	93.5	1.8	0.1	98.1	2.5	8.5	89
105	***45.8 dπ***	**43.9**	**10.3**	***72.3 dπ***	**21.9**	**5.8**	27.0 dπ	66.4	6.6
104	*69.5 dσ*	*8.6*	*21.9*	18.1 $\pi - \sigma$	77.6	4.3	***66.2 dσ***	**7.6**	**26.2**
103	*71.9 dδ*	*12.8*	*15.3*	*60.6* $\pi + \sigma$	*18.3*	*21.1*	*46.2 dπ*	*40.1*	*13.7*
102	30.4 dπ	61.3	8.3	*47.3 dδ*	*45*	*7.7*	*70.2 dδ*	*14.9*	*14.9*
101	5.2	92.4	2.4	13.6 dδ	83.1	3.3	0.2	99.6	0.2
100	3.3	91.5	5.2	0.7	99.1	0.2	3.4 *dδ*[c]	95.6	1
99	0	99.9	0.1	13.4 dδ	82.6	4	1.3	1.2	97.5
98	0	99.9	0.1	2.9	95	2.1	2.3	3.1	94.6

[a] The HOMO (or SOMO) is in bold type; mainly Ru, i.e., the "t_{2g}", orbitals are shown in italics. [b] For these complexes in which there is a strong metal−alizarin π interaction, the d_{xz} and d_{yz} orbitals combine in- and out-of-phase to give orbitals which are labeled dπ and dδ. The orbital labels refer to the Ru component only; orbital 104 in the Ru^{III} species is largely an alizarinate(2−) π orbital even though the Ru component has some σ character. [c] Orbital 96 is also dδ (see text and Table 4).

character) in all three complexes, but there is significant back-donation to the LUMO, free ligand 44, in $QQ(Ru^{II}$-1,2). Mixing of the filled 4d levels with bpy(π) levels is about the same as in the 1,9-series, with around 20% bpy character in d_{xy} (dσ) and from 6% to 15% in dπ and dδ.

$QCat^{2-}(Ru^{II}$-1,2). The LUMO and LUMO + 1 of the complex are bpy(π_1*), with the lowest $QCat^{2-}$(π*) about 0.2 eV higher in energy. The HOMO − 1 and HOMO − 2 are clearly "t_{2g}" levels with about 70% d character and are mainly d_{xy} (σ with respect to $QCat^{2-}$) and dδ, respectively. dπ is extensively mixed with the highest occupied π level of $QCat^{2-}$ (44) giving a pair of orbitals (HOMO and HOMO − 3 of the complex, 105 and 102). The Ru(dπ) character is calculated to be higher, (46% compared with 30%) in the antibonding combination (HOMO), but the HOMO has almost as much $QCat^{2-}$ character (44%) as it does Ru(dπ). The HOMO − 3 is more clearly designated as mainly $QCat^{2-}$(π) (61%). This situation is very different from that of the isoelectronic $QCat^{2-}(Ru^{II}$-1,9) in which the same two fragments, $[Ru(bpy)_2]^{2+}$ and $QCat^{2-}$, are being brought together (see above). Possibly, the Ru^{2+} in the 1,2-position tends to localize the negative charge on the 1,2- oxygen atoms and away from the naphthoquinone fragment, leading to a favorable situation for mixing between filled $QCat^{2-}$ levels and Ru valence orbitals.

$QCat^{2-}(Ru^{III}$-1,2). This complex is the only one reported here in which the oxidation state description is not completely clear since it could also be $QSq^{-}(Ru^{II}$-1,2). In addition to our ROHF calculation, we have performed a UHF calculation using ZINDO, and a density functional theory calculation. Both the UHF and DFT calculations localize the unpaired electron on the ligand rather than the metal, which suggests that the two possibilities may be very similar in energy. It is likely that if they are similar the more polar $QCat^{2-}(Ru^{III}$-1,2) structure may be stabilized in solution by polar solvents; the complex is somewhat solvatochromic, although the lowest energy band is not. The ROHF result reported here is in agreement with the EPR result and gives reasonable agreement with the electronic spectrum.

In $QCat^{2-}(Ru^{III}$-1,2), the d levels are stabilized relative to the $QCat^{2-}$ orbitals, and the SOMO − 1 is now $QCat^{2-}$-based (78%). As in the $(Ru^{III}$-1,9) complex, the calculated SOMO energy is lower than that of several fully occupied orbitals, and it has mostly d character, 72%, compared to 87% in the 1,9- Ru^{III} complex. Mainly on the basis of calculated d-orbital coefficients, and supported by the data for mixing with bpy and the intensities of the various charge-transfer transitions, the character of each Ru(t_{2g})-based MO is inferred in Table 2. The first three unoccupied levels are all bpy(π*)-based, with the $QCat^{2-}$ π* lying close in energy to bpy(π_2*).

In contrast to $QCatH^{-}(Ru^{III}$-1,9), the SOMO, orbital 105, in $QCat^{2-}(Ru^{III}$-1,2) is a Ru(dπ) level. Its calculated energy is just below that of the HOMO − 4. Orbital 104 is mainly ligand, and 103 is mainly metal. These are expected to have π and σ character, respectively, but it appears from examination of the Ru(d) coefficients that the Ru(d) components of these orbitals have mixed π and σ character. The ligand component of orbital 104 is, however, clearly π in nature. Both 103 and 102 (Ru(dδ) contain significant ligand character.

$QQ(Ru^{II}$-1,2). Upon further oxidation to $QQ(Ru^{II}$-1,2), the metal d orbitals are again stabilized, and the orbitals of the "t_{2g}" set, which are now all filled, have 46−70% Ru(4d) character. Compared to the above $QCat^{2-}(Ru^{III}$-1,2) species, there has been a significant internal electronic rearrangement due to the oxidation; the alizarinate ligand has lost two

electrons, and the metal has gained one. The largest amount of mixing is between dπ and the LUMO of QQ (alizarin 44), which form the HOMO − 1 (46% d; dπ + L) and the LUMO of the complex (27% d; L − dπ). However, this interaction is quite dependent upon the Ru−O bond length, which changes with different values of β(4d). When a shorter Ru−O length is obtained by using $\beta = -20$ eV in the calculation, the HOMO − 1 is only 60% dπ and the LUMO of the complex then has 16% d character. We have not observed such a significant dependence of mixing upon bond length for any other species here.

Interestingly, the strong mixing of the alizarin 44 and dπ is very similar (the percentages are similar but reversed) to the situation in the reduced analogue, $QCat^{2-}(Ru^{II}$-1,2), in which these same orbitals mix to form the HOMO and HOMO − 3. The LUMO lies 2 eV lower in energy than the bpy(π_1*) levels and the higher QQ(π*) level (#45 of the free ligand); thus, there is little back-donation to these orbitals compared to that to the LUMO.

Comparison of the Two Series. Overall, in the 1,2-series, there is a higher level of metal−ligand orbital mixing or covalency between Ru and alizarinate valence orbitals than occurs in the 1,9-series. A crude way of comparing this is to look at the three orbitals in the valence set which have the most d character and to add up the total percentage d orbital contribution to these orbitals, [Σ(%d)]. In a hypothetical complex with purely electrostatic bonding, this would sum to 300% for the three orbitals of the "t_{2g}" set. Any decrease from 300% represents the mixing (covalency) with either filled or empty (π back-donation) ligand orbitals. The amount of overall mixing in the 1,2-series stays relatively constant upon oxidation, the percentages being 187%, 180%, and 183% for $QCat^{2-}(Ru^{II}$-1,2), $QCat^{2-}(Ru^{III}$-1,2), and QQ-(Ru^{II}-1,2), respectively. In the 1,9-series, the percentages are 213% for $QCatH^{-}(Ru^{II}$-1,9), 204% in $QCat^{2-}(Ru^{II}$-1,9), and 201% in $QCat^{2-}(Ru^{III}$-1,9). In all Ru^{II} cases, the mixing is mainly with the π orbital that forms the HOMO of alizarin (44), and which in QQ(Ru^{II}-1,2) is a π* orbital.

The splitting of the "t_{2g}" set in the Ru^{II} species is small, around 0.2 eV, in the 1,9-series and, due to the increased mixing, slightly larger in $QCat^{2-}(Ru^{II}$-1,2) and in QQ(Ru^{II}-1,2) where the values are 0.35 and 0.31 eV, respectively.

$QCat^{2-}(Ru^{II}$-1,2) exhibits a higher degree of metal−ligand mixing than the isoelectronic $QCat^{2-}(Ru^{II}$-1,9). Since the energy differences between the orbitals of the $Ru(bpy)_2^{2+}$ fragment and those of $QCat^{2-}$ in the two species are the same, possible factors one might consider here are the symmetry and overlap (coefficients at the coordinating oxygen atoms) of the valence orbitals, geometry (five-membered vs six-membered chelate rings), and the overall electron density on the coordinating oxygen atoms. The largest degree of back-bonding to the orbital that forms the LUMO in alizarin (45) occurs in $QCat^{2-}(Ru^{II}$-1,9) for a δ type of interaction in a six-membered chelate ring, whereas the strongest back-bonding overall is to alizarin 44 in QQ(Ru^{II}-1,2), for a π type of interaction in a five-membered chelate ring. Therefore, neither the symmetry nor the geometry is likely to be the determining factor. As we suggested above, the difference is probably simply because the Ru^{2+} in the 1,2-position localizes the negative charge on the 1,2-oxygen atoms which promotes mixing between filled $QCat^{2-}$ π levels and Ru valence orbitals. The 1,2-coordinated complex, from experiment, is more thermodynamically stable in solution than the 1,9-isomer. The ligand in the 1,9-species has a less polar and more delocalized structure due to the overlap of the metal with both a (formally) quinone and a catecholate oxygen atom.

We also note that the lowest alizarinate π* (45 in the free ligand) lies close to bpy(π_1*) in all species (within 0.1−0.5 eV) except $QCat^{2-}(Ru^{III}$-1,2) in which it lies close to bpy-(π_2*). It lies slightly above the bpy(π_1*) levels in the complexes of alizarinate(2−) and slightly below in complexes of alizarinate(1−). This has an impact on the relative MLCT energies for transitions to alizarinate and to bipyridine.

Electronic Spectroscopy

Free Ligand. Alizarin has a solvatochromic low energy band (22800 cm^{-1} in ethanol, moving to higher energies in aprotic solvents)[34] which our calculations assign as a $\pi \rightarrow \pi$* transition from HOMO to LUMO (44 and 45, respectively). This transition has some charge transfer character from the 1,2-dihydroxy fragment to the 9,10-quinone group due to the nature of the orbitals involved, in agreement with most of the previous assignments;[35] it has also[36] been assigned as n $\rightarrow \pi$*. There is a weaker higher energy band at 29400 cm^{-1} which is calculated to be a $\pi \rightarrow \pi$* transition, from HOMO − 2 to LUMO (42 $\rightarrow$ 45); this was previously assigned as a $\pi \rightarrow \pi$* transition involving either the benzenoid or quinonoid fragment. Both are involved according to our calculations. Deprotonation, which occurs at the β position in alizarin, causes significant red shifts in both the observed[37] and calculated transition energies. Similar results are obtained for 1-hydroxyanthraquinone and its anion. The band positions determined by our calculations for alizarin, 1-hydroxyanthraquinone, and the corresponding anions are all in good agreement with those experimentally observed (Table 4).

In the alizarinate dianion,[37] $QCat^{2-}$, the lowest energy band is further red-shifted to 17400 cm^{-1} in methanol.

Complexes. Electronic spectra, both observed and calculated, for the redox series of the 1,9- and 1,2-coordinated complexes are shown in Figures 6 and 7, respectively. Although, in some cases, the appearance of the observed and calculated spectra differ, the main features of the INDO/S calculated electronic spectra (CIS level) are in reasonably good agreement with those experimentally observed and with

(34) (a) El Ezaby, M. S.; Salem, T. M.; Zewail, A. H.; Issa, R. *J. Chem. Soc. B* **1970**, 1293. (b) Issa, I. M.; Issa, R. M.; Idris, K. A.; Hammam, A. M. *Egypt. J. Chem.* **1973**, 67.
(35) (a) Morton, R. A.; Earlam, W. T. *J. Chem. Soc.* **1941**, 159. (b) Peters, R. H.; Sumner, H. H. *J. Chem. Soc.* **1953**, 2101. (c) Yoshida, Z.; Takabayashi, F. *Tetrahedron* **1968**, *24*, 933. (d) Diaz, A. N. *J. Photochem. Photobiol.* **1990**, *A53*, 141.
(36) Bakola-Christianopoulou, M. N. *Polyhedron* **1984**, *3*, 729.
(37) Issa, I. M.; Issa, R. M.; Idris, K. A.; Hammam, A. M. *Ind. J. Chem.* **1976**, *14B*, 117.

Table 4. Observed and Calculated Electronic Spectra of Ligands and Complexes

	electronic spectrum		assignment	
compd	obsd/cm^{-1} (ϵ/1000 mol^{-1} L cm^{-1})[a]	calcd/cm^{-1} (f)[b]	type of transition[c]	orbitals
$QCatH_2$[d,e]	22800 (8.5)	24850 (0.3)	$QCatH_2(\pi \rightarrow \pi^*)$	44 → 45
(HOMO = 44)	29400 (5.0)	27950 (0.02)	$QCatH_2(\pi \rightarrow \pi^*)$	42 → 45
$QCatH^-$[d,f]	18300 (3.4)	22200 (0.5)	$QCatH^-(\pi \rightarrow \pi^*)$	44 → 45
(HOMO = 44)	30300 (5.1)	27200 (0.03)	$QCatH^-(\pi \rightarrow \pi^*)$	42 → 45
QOH[g,h]	24900 (5.5)	25100 (0.3)	$QOH(\pi \rightarrow \pi^*)$	41 → 42
	30600 (3.3)	29750 (0.02)	$QOH(\pi \rightarrow \pi^*)$	39 → 42
QO^-[g,h]	20300 (5.0)	19000 (0.3)	$QO^-(\pi \rightarrow \pi^*)$	41 → 42
$QCatH^-(Ru^{II}\text{-}1,9)$[g]	15000sh (1.7)	16300 (0.03)	$Ru(d_{xz}) \rightarrow QCatH^-(\pi^*)$	81% 105 → 106
(HOMO = 105)	18200 (9.8)	19000 (0.3)	$Ru(d_{yz}) \rightarrow QCatH^-(\pi^*)$	67% 103 → 106
	20400sh (7.8)	19450 (0.1)	$Ru(d_{xy}) \rightarrow bpy(\pi_1^*)$	25% 104 → 107
			$Ru(d_{yz}) \rightarrow bpy(\pi_1^*)$	36% 103 → 108
		20050 (0.1)	$Ru(d_{yz}) \rightarrow bpy(\pi_1^*)$	71% 103 → 107
	22600sh (6.5)	25050 (0.1)	$QCatH^-(\pi \rightarrow \pi^*)$	89% 102 → 106
	27900 (6.7)	27050 (0.2)	$Ru(d_{xy}) \rightarrow bpy(\pi_2^*)$	37% 104 → 109
			$Ru(d_{xz}) \rightarrow bpy(\pi_2^*)$	52% 105 → 110
		27300 (0.06)	$Ru(d_{xy}) \rightarrow bpy(\pi_2^*)$	28% 104 → 109
			$Ru(d_{xy}) \rightarrow bpy(\pi_2^*)$	49% 104 → 110
		28050 (0.07)	$Ru(d_{yz}) \rightarrow bpy(\pi_2^*)$	60% 103 → 109
		28450 (0.1)	$QCatH^-(\pi \rightarrow \pi^*)$	78% 101 → 106
$QCat^{2-}(Ru^{II}\text{-}1,9)$[g]	15100sh (4.3)	14800 (0.1)	$QCat^{2-}(\pi) \rightarrow bpy(\pi_1^*)$	44% 105 → 107
(HOMO = 105)	18600 (12.1)	15500 (0.1)	$QCat^{2-}(\pi \rightarrow \pi^*)$	62% 105 → 108
		16850 (0.07)	$Ru(d_{xy}) \rightarrow bpy(\pi_1^*)$	44% 104 → 107
		17950 (0.1)	$Ru(d\delta) \rightarrow bpy(\pi_1^*)$	60% 102 → 106
		21000 (0.07)	$Ru(d\pi) \rightarrow QCat^{2-}(\pi^*)$	25% 103 → 108
		23300 (0.2)	$Ru(d_{xy}) \rightarrow bpy(\pi_2^*)$	26% 104 → 109
			$Ru(d\delta) \rightarrow QCat^{2-}(\pi^*)$	41% 102 → 108
	27300 (7.7)	24550 (0.1)	$Ru(d_{xy}) \rightarrow bpy(\pi_2^*)$	47% 104 → 109
		25200 (0.1)	$Ru(d\delta) \rightarrow bpy(\pi_2^*)$	55% 102 → 109
		26800 (0.1)	$Ru(d\delta) \rightarrow bpy(\pi_2^*)$	22% 102 → 110
			$QCat^{2-}(\pi \rightarrow \pi^*)$	23% 105 → 114
		28150 (0.09)	$Ru(d\pi) \rightarrow bpy(\pi_2^*)$	33% 103 → 110
			$Ru(d\delta) \rightarrow bpy(\pi_3^*)$	33% 102 → 111
$QCatH^-(Ru^{III}\text{-}1,9)$[i]	10600 (1.5)	12900 (0.003)	$QCatH^-(\pi \rightarrow \pi^*)$	77% 104 → 106[j]
(SOMO = 105)	18000sh	18000 (0.04)	$QCatH^-(\pi) \rightarrow Ru(d\delta)$	57% 104 → 105
	21400 (5.2)	21550 (0.08)	$QCatH^-(\pi \rightarrow \pi^*)$	78% 104 → 106[j]
	25000 rising abs	25300 (0.05)	$Ru(d\sigma) \rightarrow bpy(\pi_1^*)$	28% 103 → 107[k]
		25600 (0.1)	$Ru(d\sigma) \rightarrow bpy(\pi_1^*)$	30% 103 → 108[k]
		25700 (0.07)	$Ru(d\delta) \rightarrow QCatH^-(\pi^*)$	26% 102 → 106
		27050 (0.1)	$Ru(d) \rightarrow bpy(\pi_1^*)$	none > 20%
			$bpy(\pi \rightarrow \pi^*)$	
	peak ~ 28000	27250 (0.08)	$Ru(d) \rightarrow bpy(\pi_1^*)$	none > 20%
			$Ru(d) \rightarrow QCatH^-(\pi^*)$	
		28750 (0.1)	$QCatH^-(\pi \rightarrow \pi^*)$	29% 101 → 106
		29400 (0.1)	$QCatH^-(\pi \rightarrow \pi^*)$	33% 100 → 106
$QO^-(Ru^{II}\text{-}1,9)$[g]	14600 (1.8)	15700 (0.04)	$Ru(d_{xz}) \rightarrow QO^-(\pi^*)$	83% 102 → 103
(HOMO = 102)	18000 (13.0)	18750 (0.3)	$Ru(d_{xy}) \rightarrow bpy(\pi_1^*)$	24% 101 → 105
			$Ru(d_{yz}) \rightarrow QO^-(\pi^*)$	53% 100 → 103
		19000 (0.1)	$Ru(d_{yz}) \rightarrow bpy(\pi_1^*)$	36% 100 → 105
	19600sh (10.6)	19650 (0.09)	$Ru(d_{yz}) \rightarrow bpy(\pi_1^*)$	69% 100 → 104
	23600 (9.4)	27100 (0.4)	$QO^-(\pi \rightarrow \pi^*)$	74% 99 → 103
	27600 (9.1)	26200 (0.1)	$Ru(d_{xy}) \rightarrow bpy(\pi_2^*)$	54% 101 → 106
			$Ru(d_{xz}) \rightarrow bpy(\pi_2^*)$	38% 102 → 107
		27250 (0.1)	$Ru(d_{yz}) \rightarrow bpy(\pi_2^*)$	57% 100 → 106
$QCat^{2-}(Ru^{II}\text{-}1,2)$[g]	15600 (12.0)	16800 (0.2)	$Ru(d_{xy}) \rightarrow bpy(\pi_1^*)$	31% 104 → 106
			$Ru(d\delta) \rightarrow bpy(\pi_1^*)$	52% 103 → 106
HOMO = 105	17500 (12.0)	19100 (0.08)	$Ru(d_{xy}) \rightarrow bpy(\pi_1^*)$	31% 104 → 107
			$Ru(d\delta) \rightarrow bpy(\pi_1^*)$	35% 103 → 107
		21900 (0.3)	$Ru(d\pi) \rightarrow QCat^{2-}(\pi^*)$	54% 105 → 108
		22050 (0.1)	$QCat^{2-}(\pi \rightarrow \pi^*)$	36% 100 → 108
	27900 (11.0)	23250 (0.07)	$Ru(d\pi) \rightarrow bpy(\pi_2^*)$	59% 105 → 110
		23550 (0.1)	$Ru(d_{xy}) \rightarrow bpy(\pi_2^*)$	61% 104 → 109
		24050 (0.06)	$Ru(d\delta) \rightarrow bpy(\pi_2^*)$	63% 103 → 109
		25150 (0.05)	$Ru(d_{xy}) \rightarrow bpy(\pi_2^*)$	22% 104 → 110
			$Ru(d\pi) \rightarrow bpy(\pi_3^*)$	35% 105 → 111
$QCat^{2-}(Ru^{III}\text{-}1,2)$[g]	10600 (8.2)	12220 (0.2)	$QCat^{2-}(\pi) \rightarrow Ru(d\pi)$	68% 104 → 105
SOMO = 105	15000 (4.5)	18300 (0.02)	$QCat^{2-}(\pi \rightarrow \pi^*)$	50% 104 → 109[l]
			$Ru(d\pi) \rightarrow QCat^{2-}(\pi^*)$	23% 105 → 109
		20400 (0.02)	$Ru(d\pi/\sigma) \rightarrow bpy(\pi_1^*)$	34% 103 → 107[k]
		20700 (0.01)	$QCat^{2-}(\pi) \rightarrow Ru(d\pi)$	24% 99 → 105
			$QCat^{2-}(\pi \rightarrow \pi^*)$	20% 99 → 109
	23400 (5.6)	23050 (0.09)	$Ru(d\pi/\sigma) \rightarrow bpy(\pi_1^*)$	36% 103 → 106[k,l]
		27400 (0.2)	$QCat^{2-}(\pi \rightarrow \pi^*)$	59% 104 → 109[l]

Table 4 (Continued)

compd	electronic spectrum: obsd/cm^{-1} (ϵ/1000 mol^{-1} L cm^{-1})[a]	electronic spectrum: calcd/cm^{-1} (f)[b]	assignment: type of transition[c]	assignment: orbitals
QQ(Ru^{II}-1,2)[m]	15900 (10.3)	16800 (0.8)	Ru(dπ) → QQ(π*)	91% 103 → 105
HOMO = 104		22400 (0.07)	QQ(π → π*)	39% 100 → 105
				27%96 → 105
				22% 101 → 105
	26700 (6.0)	24550 (0.08)	Ru(d$_{xy}$) → bpy(π_1*)	71% 104 → 106
		26800 (0.07)	Ru(dδ) → bpy(π_1*)	78% 102 → 106

[a] Bands with energies below 30000 cm^{-1} are listed. [b] Transitions with calculated $f \geq 0.05$ are included; weaker transitions are listed where they are needed in order to explain the spectra. [c] Where two or more transitions are listed for the same calculated energy, these are components of the same state resulting from configuration interaction. Only contributions ≥20% are listed. [d] Exptl spectrum in ethanol. [e] ϵ value from ref 30b. [f] Spectrum run of tetraethylammonium salt. [g] Exptl spectrum in methanol. [h] Exptl data from ref 31b. [i] Exptl spectrum in acetonitrile. [j] Calcd transitions at 12900 and 21500 cm^{-1} are different excited states involving the same orbitals. See text. [k] Several other components have Ru(d) → bpy(π*) character. [l] Percentage is the sum of contributions from two excited states involving the same orbitals. [m] Spectrum run in dichloromethane.

those expected on the basis of previous literature,[36,38−41] electrochemical data,[42] and our earlier experience with quinonoid complexes.[1−3] The assignments in Table 4 provide the best match of calculated and observed data, as well as consistency between the various complexes.

All three Ru^{II} complexes of the 1,9-series are purple in solution and show an intense band in the 15000−20000 cm^{-1} region of the spectrum with a weak lower energy shoulder below 15000 cm^{-1}. A second band which is prominent in all the Ru^{II} complexes lies around 28000 cm^{-1}. The peak positions are similar to those reported for analogous complexes of other dihydroxyanthraquinone ligands.[7a,c,e] Between these two bands there is also significant absorption, which in the QO$^-$(Ru^{II}-1,9) complex has a well-defined peak close to 24000 cm^{-1}.

Spectra of [Ru(bpy)$_2$XY]$^{n+}$ complexes in which XY is a nonchromophoric ligand show two Ru(d) → bpy(π*) metal to ligand charge transfer (MLCT) bands, generally one in the visible and one in the near-UV region, which terminate on orbitals derived from the LUMO and LUMO + 1 of bpy, respectively (labeled π_1* and π_2*).[38−40,42] Although they are designated π_1* and π_2*, the orbitals are not purely those of the free bipyridine ligand but are distorted due to mixing with other bipyridine orbitals and alizarin orbitals. Some mixing of bipyridine π_1* and π_3* occurs in most complexes because these two orbitals have the same symmetry, and mixing with alizarin π* levels occurs due to the low symmetry of these complexes. The bands due to transitions to bpy(π_1*) and bpy(π_2*) are usually separated by about 7000−8000 cm^{-1} in energy and have molar absorption coefficients around 7000 M^{-1} cm^{-1}. The bands in the visible and near-UV spectra of Ru^{II} complexes with coordinated alizarinate are more intense than in "normal" [Ru(bpy)$_2$XY]$^{n+}$ complexes because of contributions from Ru(d) → alizarinate and alizarinate π → π* bands. Indeed, it is fairly unusual in the literature to describe in detail the electronic spectra of

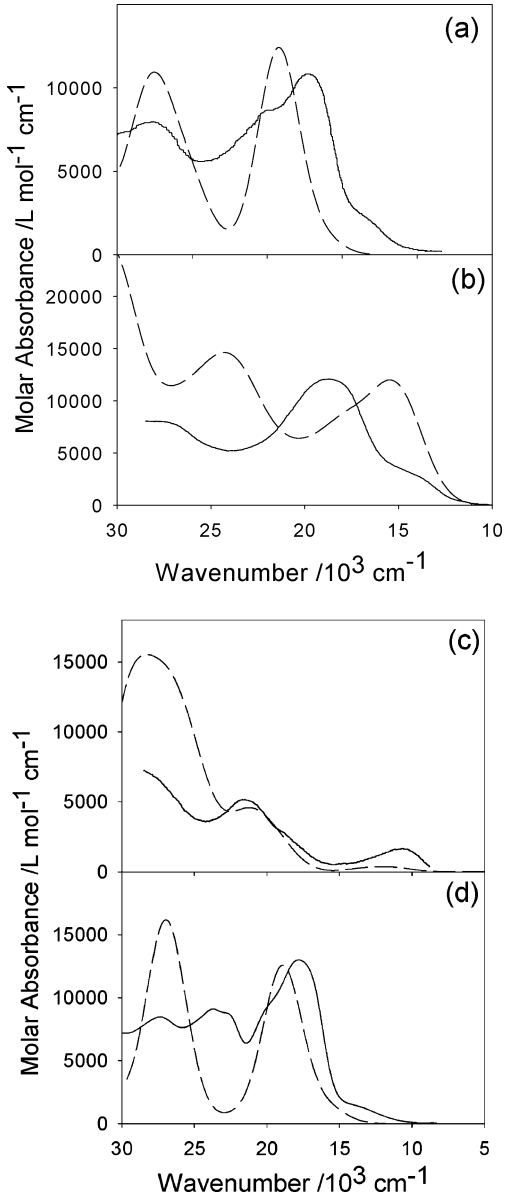

Figure 6. Observed (—) and calculated (- - -) electronic spectra of 1,9-coordinated complexes: (a) QCatH$^-$(Ru^{II}-1,9) in MeOH; (b) QCat^{2-}(Ru^{II}-1,9) in MeOH, obtained by adding trimethylamine to a solution of QCatH$^-$(Ru^{II}-1,9); (c) QCatH$^-$(Ru^{III}-1,9) in CH_3CN, obtained by addition of $NOBF_4$ (see text); (d) QO$^-$(Ru^{II}-1,9) in MeOH. Calculated spectra show the sum of all calculated transitions (not just those in Table 4). Calculated intensities are divided by two.

(38) Sullivan, B. P.; Salmon, D. J.; Meyer, T. J.; Peedin, J. *Inorg. Chem.* **1979**, *18*, 3369.
(39) (a) Sullivan, B. P.; Salmon, D. J.; Meyer, T. J. *Inorg. Chem.* **1978**, *17*, 3334. (b) Connor, J. A.; Meyer, T. J.; Sullivan, B. P. *Inorg. Chem.* **1979**, *18*, 1388.
(40) Bryant, G. M.; Fergusson, J. E.; Powell, H. K. J. *Aust. J. Chem.* **1971**, *24*, 257.
(41) Larson, L. J.; Zink, J. I. *Inorg. Chim. Acta* **1990**, *169*, 71.
(42) Dodsworth, E. S.; Lever, A. B. P. *Chem. Phys. Lett.* **1986**, *124*, 152.

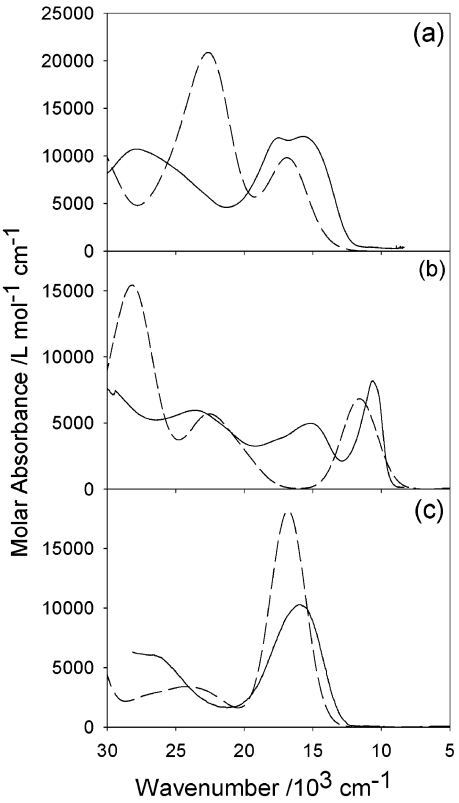

Figure 7. Observed (—) and calculated (- - -) electronic spectra of 1,2-coordinated complexes: (a) $QCat^{2-}(Ru^{II}$-1,2) in MeOH; (b) $Cat^{2-}(Ru^{III}$-1,2) in MeOH; (c) $QQ(Ru^{II}$-1,2) in CH_2Cl_2/0.2 M $TBAPF_6$, generated by controlled potential oxidation. Calculated spectra show the sum of all calculated transitions (not just those in Table 4). Calculated intensities are divided by two.

metal complexes involving ligands which are themselves strongly colored in the visible region.

$QCatH^-(Ru^{II}$-1,9). In agreement with the assignments of Gooden et al.,[7e] the intense main band in the observed spectrum is assigned as mainly $Ru(d_{yz}) \rightarrow QCatH^-$ with a weak $Ru(d_{xz}) \rightarrow QCatH^-$ transition forming the lower energy shoulder. The first higher energy shoulder comprises several overlapping Ru(d) → bpy(π_1*) transitions (Table 4, Figure 6a). To higher energy lies an alizarinate-based $\pi \rightarrow \pi^*$ transition. The ZINDO/S calculated energy of Ru(d) → bpy(π_1*) agrees extremely well with that calculated[42] (19950 cm^{-1}) from the oxidation potential, 0.73 V versus SCE.[2a] The energy of the $\pi \rightarrow \pi^*$ transition is calculated rather higher (about 3000 cm^{-1}) than the observed band: this is a reproducible pattern for these calculations, and the energy is also overestimated in calculations on the free ligand. Zink and Larson[41] have shown that the ligand $\pi \rightarrow \pi^*$ band can shift to the red in complexes compared with the free ligand, depending upon the metal and its oxidation state, but that it does not blue shift, so it is not expected to occur at energies above 22800 cm^{-1}. Highly mixed systems may be an exception to this. The difference between the observed and calculated positions of this band causes much of the visual difference between the observed and calculated spectra.

The presence of the Ru(d) → bpy(π_1*) transitions in the region around 19400 cm^{-1} is confirmed by the preliminary resonance Raman data measured at this frequency, which show several enhanced vibrations of the bipyridine ligand[1c,43] as well as bands at 1540 and 1512 cm^{-1} which must be assigned to the alizarinate ligand, and show that there are transitions involving the latter in this region as well. Near 27000 cm^{-1} lies a band encompassing Ru(d) → bpy(π_2*) and a second $QCatH^-$-based $\pi \rightarrow \pi^*$ transition. None of these designations are "pure" since all the valence orbitals have Ru(d), alizarinate, and bpy character.

$QCat^{2-}(Ru^{II}$-1,9). $QCat^{2-}(Ru^{II}$-1,9) exhibits a prominent low energy shoulder (Figure 6b) which is predicted to be an interligand charge transfer transition, LLCT. It has no counterpart in the spectra of either $QCatH^-(Ru^{II}$-1,9) or $QO^-(Ru^{II}$-1,9) and is mainly $QCat^{2-}(\pi) \rightarrow$ bpy(π_1*) in character. Similar bands have been assigned in the related complexes $[Ru(bpy)_2cat]$ (where cat = various different catechol ligands).[1a] LLCT transitions are relatively uncommon in tris-chelate complexes, and this may be the first time one has been calculated to have significant intensity.[44] The low energy shoulder may be due to either of two calculated LLCT transitions, a weak one at 14080 cm^{-1} ($f = 0.03$) or a stronger one at 14800 cm^{-1} which may alternatively contribute to the main visible region band. The higher intensity of this second band may derive from the calculated 14% alizarinate contribution to the bpy(π_1*) orbital on which the transition terminates (the LUMO + 1 of the complex). This will allow for significant overlap between the ground and excited state wave functions.

The main visible region band is very broad and clearly contains several transitions, three of which are calculated to be quite intense: the $QCat^{2-}$-based $\pi \rightarrow \pi^*$ transition (44 → 45 in the free ligand), here shifted to lower energy than in the free ligand, and two Ru(d) → bpy(π_1*) transitions. There may also be a contribution from the stronger $QCat^{2-}(\pi)$ → bpy(π_1*) transition, as mentioned above. Further, there is some contribution from Ru(d) → $QCat^{2-}(\pi^*)$, calculated to the higher energy side of the composite band. Charge transfer to catechol is not usually observed, but it arises here because of the acceptor nature of the naphthoquinone part of the ligand. There is a shift to higher energy of about 4400 cm^{-1} in the Ru(d) → $QCat^{2-}(\pi^*)$ transition relative to that in $QCatH^-(Ru^{II}$-1,9) due to the loss of the proton. Several transitions of significant intensity are calculated to contribute to the higher energy band around 27000 cm^{-1}, including Ru(d) → bpy(π_2*), Ru(d) → bpy(π_3*), and $QCat^{2-}(\pi \rightarrow \pi^*)$.

$QCatH^-(Ru^{III}$-1,9). This complex exhibits a weak, low energy band (Figure 6c) which does not appear to have a counterpart in the spectra of the related $[Ru(bpy)_2]^{3+}$ complexes of 1,4-, 1,5-, and 1,8-dihydroxyanthraquinones reported previously.[7e] In a simple localized model, the lowest band in a Ru^{III} complex would normally be assigned as ligand to metal charge transfer (LMCT) from $QCatH^-$ to Ru^{III}, on the basis of the EPR result. However, ZINDO assigns this weak band as a ligand-centered transition, $QCatH^-(\pi \rightarrow \pi^*)$,

(43) (a) Mabrouk, P. A.; Wrighton, M. S. *Inorg. Chem.* **1986**, *25*, 526. (b) Mallick, P. K.; Danzer, G. D.; Strommen, D. P.; Kincaid, J. R. *J. Phys. Chem.* **1988**, *92*, 5628.
(44) (a) Vogler, A.; Kunkely, H. *Comments Inorg. Chem.* **1990**, *9*, 201. (b) Acosta, A.; Zink, J. I.; Cheon, J. *Inorg. Chem.* **2000**, *39*, 427.

between the same orbitals, 104 → 106, as the higher band observed and calculated around 21500 cm^{-1}. Similar bands around 21000 cm^{-1} have been assigned in the literature as MLCT to dihydroxyanthraquinone.[7e] Our calculations show such transitions to occur at higher energy (see below) in the alizarin system. The spectrum is quite well represented by the calculations apart from the relative intensity of the lowest energy band. This can be improved by adding double excitations to the calculation, though the appearance of the higher energy band is then less like the observed spectrum.

The occurrence of two spin-allowed transitions between the same pair of orbitals is possible because two spin-allowed spin doublet excited states, differing in Coulombic and exchange energies, arise from coupling between orbitals 104 and 106 with the SOMO 105. Thus, we cannot make simple comparisons between the energies of ligand-centered transitions in this complex and other complexes or the free ligand. This also applies to charge transfer transitions such as Ru(d) → bpy(π_1*), and was not taken into account in our earlier discussions of related open shell systems.[1a,f,3b,i]

The expected LMCT transition is calculated to be the shoulder at 18000 cm^{-1}, with the calculation agreeing very well with experiment. This transition is quite weak, cf. the analogous transition in the 1,2-series, also 104 → 105; this is presumably due to its $\pi \rightarrow \delta$ character. Two intra-t_{2g} transitions are predicted to occur in the IR region at 1560 and 2800 cm^{-1}, but we find no evidence of them in the IR or near-IR spectrum.

The absorption rising from about 25000 cm^{-1} toward the UV region is accounted for by many calculated transitions, most of which are quite mixed in nature, i.e., with the major contributor accounting for only 20−30% of the transition. Much of this absorption has MLCT character despite the metal being Ru^{III}, and no bpy → Ru(d) LMCT transitions are calculated to occur in the visible region. The first part of this absorption is attributed to Ru(d) → bpy(π_1*) MLCT around 25000 cm^{-1}, similar in energy to that for a $Ru^{II}(bpy)_2$ complex with a strong π-acceptor attached.[1a,39] Although these transitions are heavily mixed through CI, many of the components have Ru(d) → bpy(π*) character, and this is unequivocally a reasonable description of these transitions. At very slightly higher energy, Ru(d) → $QCatH^-$(π*) MLCT transitions are calculated to occur, and around 29000 cm^{-1}, there are further internal alizarinate-based $\pi \rightarrow \pi$* bands.

In general, the observed and calculated intensities are much lower for this open shell complex than for the closed shell ones, and overall agreement between calculated and experimental spectrum is remarkably good (Figure 6c).

QO^-(Ru^{II}-1,9). The assignments in this complex are similar to those for $QCatH^-$(Ru^{II}-1,9). Both the shoulder at low energy and the main band are mainly Ru(d) → QO^-(π*). Two Ru(d) → bpy(π_1*) transitions form the shoulder around 19600 cm^{-1} and may contribute to the main band. Consistent with this, resonance Raman data exciting at 19400 cm^{-1} show vibrations of bipyridine,[1c,43] in addition to vibrations at 1657, 1531, 1500, 1424, 1232, and 1035 cm^{-1}, which are attributed to hydroxyanthraquinone.

The band around 24000 cm^{-1} (Figure 6d) is probably the equivalent of the shoulder at 22000 cm^{-1} in $QCatH^-$(Ru^{II}-1,9), i.e., QO^-($\pi \rightarrow \pi$*). The difference in energy between these two bands is about the same as the calculated shift in the $\pi \rightarrow \pi$* band, supporting their assignments as analogous transitions. Both are calculated to lie at significantly higher energies than apparently observed (the error is 3500 cm^{-1} in this case), and are also higher than expected, on the basis of the electronic spectra of the free ligand and the monoanion.[37] Here again we see a situation where several bands are resolved in the experimental spectrum but lie a little closer together in the predicted spectrum and, as a consequence, are not resolved. Zerner has commented that ZINDO seems to perform less well for oxygen-containing organic systems;[30] for example, calculated positions of n → π* transitions are often too low. Ward reports ZINDO calculations on dioxolene systems in which the calculated band energies are consistently too high.[4x] There is also precedent for the energies of $\pi \rightarrow \pi$* bands being overestimated: ZINDO gives an energy for the B band in heme which is 4000 cm^{-1} too high.[30]

$QCat^{2-}$(Ru^{II}-1,2). By contrast with the isoelectronic $QCat^{2-}$(Ru^{II}-1,9), $QCat^{2-}$(Ru^{II}-1,2) exhibits solvatochromic transitions; bands at 15600 and 17500 cm^{-1} in methanol (blue solution) (Figure 7a) shift to 14800(sh) and 16400 cm^{-1} in 1,2-dichloroethane (turquoise solution). The higher energy band, at 27900 cm^{-1} in methanol, splits into two at 25400(sh) and 27100 cm^{-1} in 1,2-dichloroethane; i.e., it appears that at least four transitions red shift in dichloroethane compared to methanol.[45] The 16000−17000 cm^{-1} band increases in energy with increasing acceptor number (AN).[46] This suggests an interaction between lone pairs of the complex and solvent, either at the quinone C═O or at the coordinated (catechol-type) oxygen atoms. The blue shift with increasing AN would be consistent with the hydrogen bonding solvent withdrawing electron density from the coordinating oxygen atoms and stabilizing the Ru orbitals, causing a blue shift in charge transfer transitions from Ru(d) to bipyridine or to alizarinate (assuming that the d orbitals are stabilized more than the $QCat^{2-}$(π*)). All except one of the major transitions calculated to occur in the visible region are MLCT, with most of these being Ru(d) → bpy(π*). However, the solvatochromism has not been investigated in detail because of the complexity of the spectrum. For the discussion below we refer to the methanol data.

The direction of the spectroscopic shift induced by hydrogen bonding solvents is opposite for this complex to that of the free ligand. In the latter, the hydrogen bonding solvent (ethanol) causes a red shift compared to other solvents; the alcoholic solvent probably raises the energy of the $QCat^{2-}$(π) donor levels by interacting with the hydroxy protons, particularly in the 2-position, causing a red shift in $QCat^{2-}$($\pi \rightarrow \pi$*) transitions. El Ezaby[34a] suggested similarly that solvent interaction with the OH group facilitated charge transfer to the anthraquinone nucleus. 2-hydroxyanthraquinones are much more solvatochromic than their 1-substituted

(45) Auburn, P. R.; Lever, A. B. P. Unpublished observations.
(46) Gutmann, V. *Electrochim. Acta* **1976**, *21*, 661.

analogues because the internal hydrogen bond formed between the 1-OH and the neighboring carbonyl is very strong and not broken by interaction with solvent molecules.[35c,47]

In agreement with the observation of two overlapping peaks of the same absorbance at low energy, two transitions of similarly high intensity, at 16800 and 21900 cm^{-1}, are calculated, along with two weaker bands in the same region. Similar energies are calculated for the main transitions by time dependent density functional theory, using the ZINDO/1 optimized structure. The lower of the main transitions is Ru(d) → bpy(π_1*), and the higher is 105 → 108 which is most simply designated as Ru(dπ) → $QCat^{2-}$(π*) though it has significant $QCat^{2-}$(π → π*) character due to the mixing of Ru(dπ) with $QCat^{2-}$(π*). That the energies do not agree well with the observed energies may result partly from the solvatochromism of this complex.

As mentioned above, charge transfer to catechol itself is not normally expected because of the relatively high energy of its LUMO, and the saturated linkage to ruthenium. However, in $QCat^{2-}$ the LUMO is lowered by the quinone and is sufficiently delocalized to allow overlap with the d orbitals. A "purer" $\pi \rightarrow \pi^*$ transition from a lower π level (100 in the complex) is also calculated at similar energy. It seems possible that the energies of both these transitions are overestimated by ZINDO/S, as we concluded for the $\pi \rightarrow \pi^*$ band in the $CatH^-$ and QO^- 1,9-coordinated complexes. This would account for much of the difference between the observed and calculated spectra (Figure 7a).

The calculated Ru(d) → bpy(π_1*) transitions in $QCat^{2-}$-(Ru^{II}-1,2) are spread over a range of about 5000 cm^{-1}, (14000−19000 cm^{-1}; some of these are weak and not listed in Table 4). These all lie under the lowest double band, with Ru(d) → bpy(π_2*) lying under the rising absorption that begins around 21000 cm^{-1}. The spread is similar for all the Ru^{II} complexes discussed here, despite the differing degrees of interaction with the ligand, and it is larger than the d(t_{2g}) orbital splitting (∼2800 cm^{-1} in this case) in all the Ru^{II} complexes. Like its isomer, $QCat^{2-}$(Ru^{II}-1,9), $QCat^{2-}$(Ru^{II}-1,2) exhibits lower lying Ru(d) → bpy(π_1*) transitions than $QCatH^-$(Ru^{II}-1,9) and QO^-(Ru^{II}-1,9) due to the greater electron density on the metal; the Mulliken charges for Ru are 0.43 and 0.46 in $QCat^{2-}$(Ru^{II}-1,2) and $QCat^{2-}$(Ru^{II}-1,9), and 0.51 and 0.50 in $QCatH^-$(Ru^{II}-1,9) and QO^-(Ru^{II}-1,9). Since there are no strong transitions to bpy from dπ, the raising of the highest d orbital energy by interaction with the $QCat^{2-}$ HOMO does not have a significant effect on the spectrum.

The energy of Ru(d) → bpy(π_1*) can also be estimated from the $Ru^{III/II}$ potential,[42] 0.06 V versus SCE, giving 16400 cm^{-1}, compared to the ZINDO value of 16800 cm^{-1}. The preliminary RR spectra measured at 19400 cm^{-1}, to the high energy side of the main pair of visible region bands, also confirm the presence of a Ru(d) → bpy(π*) transition in this region, as predicted by ZINDO/S. The resonance enhanced bands are probably all due to vibrations of the bpy ligand,[1c,43] though there is some uncertainty about the band at 1436 cm^{-1}. Most of the bpy vibrations are shifted to lower energy compared to the literature, particularly those at 1585, 1543, and 1253 cm^{-1} (cf. 1604, 1556, and 1268 cm^{-1} in ref 1c), perhaps because this complex has, according to the calculations, a larger than usual degree of back-bonding to bpy.

The counterpart of the $QCat^{2-}$(π) → bpy(π_1*) transition seen in the $QCat^{2-}$(Ru^{II}-1,9) species does not occur as a single strong transition in this species but contributes to extremely weak (not listed in Table 4 and not observed) transitions calculated to occur in the near-IR and near-UV regions.

$QCat^{2-}$(Ru^{III}-1,2). The electronic spectrum of $QCat^{2-}$-(Ru^{III}-1,2) exhibits an intense low energy band at 10600 cm^{-1}, coincidentally the same energy as the lowest band in $QcatH^-$(Ru^{III}-1,9) (Figure 7b). This is calculated to be an LMCT band, $QCat^{2-}$(π) → Ru(dπ), SOMO − 1 → SOMO. Its intensity and narrowness agree with its assignment as a transition between a mixed $QCat^{2-}$(π) and Ru(dπ) pair of orbitals, with some Ru(dσ) character as well as Ru(dπ), in the mainly $QCat^{2-}$(π) orbital (104). The next observed band is at 15000 cm^{-1}, whose energy the calculations do not reproduce well. A number of transitions are calculated to lie in the 18000−20000 cm^{-1} range where there is no observed peak. It seems likely that, as discussed above, the lowest internal $QCat^{2-}$($\pi \rightarrow \pi^*$) band energy is overestimated by about 3000 cm^{-1} and that this is the assignment of the 15000 cm^{-1} band.

Weaker absorption between the peaks at 15000 and 23400 cm^{-1} is attributed to Ru(d) → bpy(π_1*) and a mixed LMCT ($QCat^{2-}$(π) → Ru(d)) and $QCat^{2-}$($\pi \rightarrow \pi^*$) transition, and the 23400 cm^{-1} peak itself is assigned as Ru(d) → bpy(π_1*). As in the (Ru^{III}-1,9) complex, although the information in Table 4 might suggest that Ru(d) → bpy(π*) is only a small component, this is not the case since there are several CI components with this character making up the transition. A higher energy $QCat^{2-}$($\pi \rightarrow \pi^*$) transition is predicted at 27200 cm^{-1} where there is absorption, but no actual peak. No low energy, weak intra-t_{2g} transitions have been observed for this species although they are calculated to lie at 1360 and 3165 cm^{-1}.

QQ(Ru^{II}-1,2). In QQ(Ru^{II}-1,2) the main visible region transition (Figure 7c), whose energy is very well predicted by ZINDO, is calculated to be a fairly "pure" transition from the mainly Ru(dπ) HOMO − 1 to the QQ-based LUMO. These two orbitals interact strongly, and the transition is predicted to be extremely intense, though $f = 0.75$ is obviously a gross overestimate. It is common for ZINDO/S to overestimate by 2−3 times the intensity of more intense bands.[30] The calculated intensity is also very high relative to the next set of transitions around 22000−28000 cm^{-1}. This latter broad multiple absorption clearly involves several transitions and is predicted by ZINDO/S to comprise mainly QQ($\pi \rightarrow \pi^*$) and Ru(d) → bpy(π_1*) transitions, a number of which are weak and not listed in Table 4. The Ru(d) → bpy(π_1*) transitions are at rather high energy compared to those of most [Ru(bpy)$_2$XY] complexes,[38−40,42] due to the

(47) Reta, M. R.; Cattana, R.; Anunziata, J. D.; Silber, J. J. *Spectrochim. Acta* **1993**, *49A*, 903.

weak donor and strong π-acceptor nature of the deprotonated, oxidized, quinonoid alizarin ligand (typical of coordinated quinones). They are comparable in energy to those calculated for the ruthenium(III) complex, $QcatH^{-}(Ru^{III}$-1,9), and they lie close to the expected position based on the approximate oxidation potential of the complex.[42,48] The Mulliken charge calculated for the Ru in this complex is 0.57.

Summary and Conclusions

First, we find the ZINDO/S calculations, based on ZINDO/1 structures, to be helpful in indicating which types of transitions are expected in the electronic spectra, and providing reasonable energies and relative intensities, particularly for the closed shell systems. A cursory analysis of Figures 6 and 7 might indicate relatively poor agreement between the ZINDO/S predicted spectra and the experimental data for some, though not all, species. In fact, the agreement is remarkably good in all cases, allowing for the fact that the main features of the spectra are reproduced, that the experimental data sometimes resolve features which overlap in the predicted spectra, and that there appears to be, in many cases, an overestimate of the $\pi \rightarrow \pi^*$ transition energies. In general the energies of the lowest observed transitions are well reproduced, as are the Ru(d) $\rightarrow$ bpy(π^*) transitions. It appears that the errors are larger for certain types of transitions than for others, particularly where O-donor rather than N-donor ligands are involved, and this seems to be a consistent pattern in this series of complexes.

ZINDO/1 does not seem to reproduce changes in bond lengths with oxidation state very well, but in general, structural differences do not affect the calculated spectra and mixing greatly, with the exception of the Ru(d) contribution to the LUMO in the $QQ(Ru^{II}$-1,2) species. The ZINDO/1 results also seem to be noticeably better for nitrogen-donor ligands than for oxygen-donor ligands.

The most unusual transition we have observed here is the alizarinate to bipyridine transition in $QCat^{2-}(Ru^{II}$-1,9). It originates from the alizarinate HOMO and terminates on a bpy(π^*) orbital, and it is both calculated and observed to have significant intensity. LLCT transitions are common in square planar complexes where one ligand is easily reduced and the other is easily oxidized, but they are less common in other systems.[44]

The calculated positions of the main Ru(d) $\rightarrow$ bpy(π^*) bands are generally very consistent with the literature for similar complexes such as $Ru(bpy)_2(acac)$ (where acac is acetylacetonate),[40] and with energies calculated from $Ru^{III/II}$ potentials,[42] and they shift as expected when the charge on the alizarinate ligand is changed.[38−40,42] For Ru(d) $\rightarrow$ bpy(π_1^*), the calculated energies vary from around 18000 cm^{-1} in $QCat^{2-}(Ru^{II}$-1,9) to over 24000 cm^{-1} in $QQ(Ru^{II}$-1,2). The differences between the most intense Ru(d) $\rightarrow$ bpy(π_1^*) and the most intense Ru(d) $\rightarrow$ bpy(π_2^*) in each complex, around 7000−8000 cm^{-1}, are also consistent with literature data for simpler complexes.[38−40,42] There is significant configuration interaction (CI) between transitions in these low symmetry species, particularly between the different Ru(d) $\rightarrow$ bpy(π^*) transitions but also between transitions of different types and similar energies (see Table 4).

Transitions of the MLCT type from Ru(d) to alizarin occur in most species but are most intense and dominant in the spectrum in $QQ(Ru^{II}$-1,2) where there is strong mixing between Ru(dπ) and the LUMO of the doubly oxidized alizarin. Ru(d) $\rightarrow$ $QCatH^{-}(\pi^*)$ occurs at around 19000 cm^{-1} in $QCatH^{-}(Ru^{II}$-1,9) and is shifted to higher energy (22000−23000 cm^{-1}) when the ligand is deprotonated, in $QCat^{2-}(Ru^{II}$-1,9) and $QCat^{2-}(Ru^{II}$-1,2), although ruthenium is bound to a catechol fragment in the latter. When the ruthenium is formally oxidized to Ru^{III}, MLCT transitions still occur, at around 26000 cm^{-1} in the 1,9-coordinated species, and they contribute to the band at 18000 cm^{-1} in the 1,2-coordinated species.

LMCT transitions from alizarinate to ruthenium are calculated to occur at 18000 cm^{-1} in $QCatH^{-}(Ru^{III}$-1,9) and at 12000 cm^{-1} in $QCat^{2-}(Ru^{III}$-1,2), the difference showing the effect of the proton on the donor π orbital of alizarin. In general, the electronic spectra of the open shell species are remarkably well predicted by the ROHF ZINDO/S code despite the problems often encountered in analyzing such species.

The lowest alizarin-based ($\pi \rightarrow \pi^*$) transition lies around 23000 cm^{-1} in the free ligand and shifts to lower energy when the ligand is deprotonated. These energies are reasonably well reproduced for the free ligands by ZINDO/S. In the Ru^{II} complexes of $CatH^{-}$ and QO^{-}, bands assigned as $\pi \rightarrow \pi^*$ transitions of the anthraquinone ligand lie at energies very close to those in the free (fully protonated) ligands. However, in both these cases the calculated energies are significantly higher. In $QCat^{2-}(Ru^{II}$-1,9) and $QCat^{2-}(Ru^{III}$-1,9), the $QCat^{2-}(\pi \rightarrow \pi^*)$ band(s) is (are) shifted to lower energy, as occurs for the anionic free ligand, and the calculated values agree well with experiment. However, in $QCat^{2-}(Ru^{III}$-1,2) the band assigned as $QCat^{2-}(\pi \rightarrow \pi^*)$ is again lower in energy than calculated, with the observed band being at similar energy to the free ligand dianion.[37]

A detailed study of the electronic structure of these complexes indicates a higher degree of orbital mixing in $QCat^{2-}(Ru^{II}$-1,2) compared to its isomer $QCat^{2-}(Ru^{II}$-1,9), and in general for the 1,2-coordinated species compared to the 1,9-coordinated species. We conclude that this is mainly due to the "QCat" canonical form being the most favorable as it obviously is in the free ligand, and having the most available electron density for donation to ruthenium. In the QQ complex, as with other quinones, much of the metal−ligand orbital mixing is due to back-donation to the quinone ligand and involves the ligand LUMO, whereas in the other complexes the mixing mainly involves filled ligand orbitals. In all the complexes, except $QCatH^{-}(Ru^{II}$-1,9) and $QO^{-}(Ru^{II}$-1,9), the metal interacts strongly enough with the alizarinate ligand that the d orbitals are essentially hybridized as they

(48) A previously unreported irreversible oxidation occurs at 1.9 V vs SCE in $QQ(Ru^{II}$-1,2). On the basis of this $Ru^{III/II}$ potential, QQ has an E_L value[49] of 0.55 eV, compared to −0.37 for 1,2-coordinated $QCat^{2-}$, and −0.03 for $QcatH^{-}$.

(49) Lever, A. B. P. *Inorg. Chem.* **1990**, *29*, 1271.

would be in a C_{2v} system, despite the actual low symmetries (C_1) of these species.

Acknowledgment. We are indebted to the Natural Sciences and Engineering Research Council (Ottawa), and the Office of Naval Research (Washington), for financial support; to Drs. S. I. Gorelsky, C. da Cunha, Y.-H. Tse, and R. A. Metcalfe for valuable discussions, Dr. P. R. Auburn for the initial synthesis of the 1,2-coordinated complex, Dr. B. Lenain for RR measurements, Dr. J. Reimers for providing INDO/S code and for helpful discussions, the late Michael Zerner for supplying his developmental ZINDO code; and to the Johnson-Matthey Company for the loan of $RuCl_3$. A.B.P.L. thanks the Canada Council for the Arts for a Killam Fellowship.

Supporting Information Available: Tables of eigenvalues for orbitals 90−120, total energies of the complexes, atomic bond distances in the optimized structures, and xyz coordinates. This material is available free of charge via the Internet at http://pubs.acs.org.

IC035370D